DOI:
10.1681/ASN.2017050544

Document Version
Peer reviewed version

JASN

Collectin-11 is required for the development of renal tubulointerstitial fibrosis

Journal:	*Journal of the American Society of Nephrology*
Manuscript ID	JASN-2017-05-0544.R2
Manuscript Type:	Original Article - Basic Research
Date Submitted by the Author:	n/a
Complete List of Authors:	Wu, Weiju; King's College London, Department of Innate Immunity, MRC Centre for Transplantation Liu, Chengfei; Xi'an Jiaotong University, Core Research Laboratory, the Second Affiliated Hospital, , School of Medicine Farrar, Conrad; King's College London, Nephrology and Transplantation Ma, Liang; King's College London, Department of Innate Immunity, MRC Centre for Transplantation Dong, Xia Sacks, Steven; King's College London, Nephrology & Transplantation Li, Ke; Xi'an Jiaotong University, Core Research Laboratory, The Second Affiliated Hospital, School of Medicine Zhou, Wuding; King's College London, MRC Centre for Transplantation
Keywords:	collectin 11, renal fibrosis, leukocyte migration, renal fibroblast proliferation, carbohydrate ligands

Collectin-11 is required for the development of renal tubulointerstitial fibrosis

Weiju Wu[1], Chengfei Liu[2], Conrad A. Farrar[1], Liang Ma[1], Xia Dong[1], Steven S. Sacks[1], Ke Li[2] & Wuding Zhou[1]

[1]Medical Research Council (MRC) Centre for Transplantation, King's College London, Guy's Hospital, UK

[2]Core Research Laboratory, the Second Affiliated Hospital, School of Medicine, Xi'an Jiaotong University, China

Condensed title: Collectin-11 promotes renal fibrosis

Address for correspondence:
Professor Wuding Zhou
MRC Centre for Transplantation
King's College London
5th Floor Tower Wing
Guy's Hospital
Great Maze Pond
London SE1 9RT
UK
Telephone: +44 (0)20 7188 1528
wuding.zhou@kcl.ac.uk

Authorship note:

W. Wu and C. Liu are co-first authors. K. Li and W. Zhou are equal senior authors.

Abstract

Collectin-11 is a recently described soluble C-type lectin, a pattern recognition molecule of the innate immune system that has distinct roles in host defense, embryonic development as well as acute inflammation. However, little is known to date regarding its role in tissue fibrosis. Here, we report a pathogenic role for collectin-11 in renal tubulointerstitial fibrosis. Compared to wild-type littermate controls we found that collectin-11$^{-/-}$ mice had significantly reduced renal chronic inflammation and tubulointerstitial fibrosis, as evidenced by reduced renal functional impairment, tubular injury, renal leukocyte infiltration, renal tissue inflammation/fibrogenesis and collagen deposition in the kidneys following native renal ischemia/reperfusion (IR) injury. Similarly, collectin-11$^{-/-}$ kidney grafts displayed significantly reduced tubular injury and collagen deposition compared with collectin-11$^{+/+}$ kidney grafts following syngeneic kidney transplantation. Mechanistic analyses revealed that collectin-11has potent effects in promoting leukocyte migration and stimulating renal fibroblast proliferation *in vitro* in a carbohydrate-dependent manner. Our findings demonstrate a previously unknown pathogenic role for collectin-11 in the development of tubulointerstitial fibrosis and suggest that local presence of collectin-11promotes the fibrosis through its effects on leukocyte chemotaxis and renal fibroblast proliferation, in addition to triggering complement activation and acute inflammation. It provides a novel insight into pathogenesis of tubulointerstitial fibrosis and will have implications for chronic kidney disease mediated by other causes.

Introduction

Chronic kidney disease (CKD) is a progressive loss of kidney function over a period of time. CKD was ranked 19th in the list of causes for global deaths in 2013. Prevalence of CKD is estimated to be 8-16% worldwide and expected to rise substantially in the coming decades.[1] Acute kidney injury (AKI) is one of the main causes of CKD, among other causes (e.g. diabetes and hypertension, infectious glomerulonephritis, renal vasculitis).[2] Renal fibrosis is the principal process underlying of the progression of CKD to end-stage renal disease (ESRD). Progressive tubulointerstitial fibrosis is the final common pathway for all kidney diseases leading to ESRD. As there are currently no specific treatments for tubulointerstitial fibrosis, a deeper understanding of molecular and cellular basis of tubulointerstitial fibrosis will be beneficial to the development of effective strategies that diminish or even reverse tubulointerstitial fibrosis in CKD.

Renal tubulointerstitial fibrosis is characterized by progressive loss of renal function and renal histological lesions mainly including inflammatory cell infiltration, tubule damage (e.g. tubular atrophy,

tubule loss) and accumulation of extracellular matrix (collagen deposition).[3] The pathogenesis of tubulointerstitial fibrosis is complex, involving multiple cell types and molecular pathways.[4, 5] The major cell type involved in production of extracellular matrix (ECM) is the myofibroblast which produces a large amount of collagen I (Col I) and fibronectin (FN).[6, 7] Myofibroblasts mainly differentiate from renal interstitial fibroblasts. Other types of cells in the kidney such as bone marrow-derived fibrocystic, stromal mesenchymal cells, and renal tubular epithelial cells have been reported to be able to transform into myofibroblasts.[8] The inflammatory microenvironment of the kidney following renal injury is thought to play a key role in determining the dynamic balance between tissue destruction and repair, and ongoing inflammation including inflammatory cell infiltration and local production/release of pro-inflammatory and pro-fibrogenic molecules drives the fibrotic process.[9]

Collectins (soluble collagenous C-type lectins) are a part of the innate immune system.[10, 11] Well described collectins include mannose-binding lectin (MBL) and lung surfactant proteins (e.g. SP-A). They function as pattern recognition receptors that bind to carbohydrates or carbohydrate moieties on the surface of pathogens and host cells, and accordingly have important roles both in host defence and the regulation of cellular responses.[12-14] Collectin-11 (CL-11; also known as CL-K1 and encoded by *COLEC11*) is a recently described member of the collectin family and displays structural similarities with MBL, SP-A and SP-D. CL-11 consists of a carbohydrate recognition domain (CRD), followed by a neck region and a collagen-like region and is known to bind to various molecules/molecular patterns (e.g. monosaccharides, mannose-containing glycans, LPS, DNA, microorganisms), via interaction with the CRD.[15-18] CL-11 has a wide tissue distribution; high-level expression was found in the kidney, liver and adrenal gland.[17] CL-11 is known to play important roles in embryonic development and host defense,[19, 20] while relatively little is currently known about the pathogenic roles of CL-11.

Our recent work in a murine model of renal ischemia/reperfusion (IR) injury demonstrated that CL-11 has a pathogenic role in AKI.[21] However, the impact of CL-11 on chronic renal inflammation and tissue fibrosis is presently unknown. Such information will improve our understanding of diverse functions of CL-11 in the pathogenesis of renal injury. Previous studies have shown that many factors (e.g. Wnt pathway, Hedgehog pathway, Gremlin1, TGF-β) responsible for the control of embryonic devolvement are also key players in tissue repair and fibrosis.[22-25] Given the role of CL-11 in embryonic devolvement and its potential for regulation of diverse cellular processes, we hypothesized that CL-11 also plays important roles in renal fibrosis. In the present study, we employed two models (i.e. bilateral renal IR injury and syngeneic kidney transplantation) in CL-11$^{-/-}$ mice to interrogate the role of CL-11 in the development of renal tubulointerstitial fibrosis. We also performed a series of *ex vivo* analyses and *in vitro* experiments (using primarily cultured murine renal fibroblasts and peritoneal

exudate leukocytes) to explore the mechanisms by which CL-11 promotes renal fibrosis. Our data demonstrate a pathogenic role for CL-11 in promoting chronic renal inflammation and tubulointerstitial fibrosis. The mechanism by which CL-11 mediates pro-fibrotic effects involves both the promotion of leukocyte migration and stimulation of renal fibroblast proliferation.

Results

CL-11 mediates tubule damage and renal function impairment in the late phase of renal IR injury

To assess the impact of CL-11 on renal function and histological injury during the late phase of renal IR injury, we induced bilateral renal ischemia (30 min) in CL-11$^{+/+}$ and CL-11$^{-/-}$ mice, followed by reperfusion up to 7 days. Renal function was evaluated at 2 and 7 days post-reperfusion by measuring blood urea nitrogen (BUN), and significantly lower BUN levels were observed in CL-11$^{-/-}$ mice at both time points, compared with CL-11$^{+/+}$ mice (Fig. 1a), indicating there was less impairment of renal function in CL-11$^{-/-}$ mice. CL-11$^{-/-}$ mice also displayed less severe renal histological lesions (i.e. proximal tubule brush border loss, tubule necrosis, tubule atrophy, protein casting, cellular infiltration in the cortical medullary junction) at 7 days post-reperfusion when compared to CL-11$^{+/+}$ controls (Fig. 1b). Histopathological scores also confirmed the attenuation of renal lesions in the CL-11$^{-/-}$ mice (Fig. 1c). Collectively, these results demonstrate that CL-11 deficiency not only protects mice from AKI, but also reduces tubular damage and renal function impairment in the late phase of IR injury.

CL-11 is required for accumulation of ECM in the kidney following renal IR

Accumulation of ECM (collagen deposition) in the kidney following renal IR injury (7 days post-reperfusion) was initially assessed by Sirius red staining. Compared to CL-11$^{+/+}$ mice, CL-11$^{-/-}$ mice displayed a significant reduction of Sirius red staining in the tubular interstitium (Fig. 2a, 2b). Accumulation of ECM was further analyzed by immunohistochemistry for detection of ECM proteins (COL I, FN) and cytoskeletal protein (vimentin). Compared to CL-11$^{+/+}$ mice, CL-11$^{-/-}$ mice exhibited markedly reduced COL I and FN deposition and vimentin expression in the tubular interstitium, as well as a better preservation of proximal tubular epithelial cells (assessed by lotus tetragonolobus [LTL] staining) (Fig. 2c). Intrarenal expression of COL I and FN was also analyzed by RT-qPCR. Significantly lower mRNA levels of these molecules were observed in the kidneys from CL-11$^{-/-}$ mice, compared to CL-11$^{+/+}$ controls (Fig. 2d). Taken together, these observations demonstrate that CL-11

deficiency reduces accumulation of ECM and proximal tubule damage, which corresponds well with of a reduction in renal function impairment and histological scores described in figure 1.

CL-11 is required for renal inflammatory cell infiltration, tissue inflammation and fibrogenesis following renal IR

An influx of inflammatory cells is a hallmark of tubulointerstitial fibrosis. We therefore examined inflammatory cell infiltration in the kidneys of CL-11$^{+/+}$ and CL-11$^{-/-}$ mice following the induction of renal IR injury using flow cytometry and immunohistochemistry. Flow cytometry analysis of renal cell suspensions showed that under normal conditions, there was no significant difference in basal levels of leukocytes between CL-11$^{+/+}$ and CL-11$^{-/-}$ mice (data not shown). Following induction of renal IR injury, leukocyte infiltration increased in both groups of mice. However, CL-11$^{-/-}$ mice had significantly lower numbers of CD45^{+} (total leukocytes) in the kidneys at 2 and 7 days post-reperfusion, when compared to CL-11$^{+/+}$ controls (Fig. 3a, 3b). As the infiltrating leukocytes (CD45^{+}) in the kidney post-reperfusion were mainly composed of Ly6G^{+} (neutrophil) and Ly6G^{-}F4/80^{+} (monocyte/macrophage [MO/MΦ]), we further analyzed the infiltration of these two types of cells. CL-11$^{-/-}$ mice had lower numbers of both Ly6G^{+} (neutrophil) and Ly6G^{-}F4/80^{+} (monocyte/macrophage [MO/MΦ]) in the injured kidneys, which was more clearly demonstrated at day 2 for neutrophil and day 7 for MO/MΦ (Fig. 3a, 3b). Immunohistochemistry also demonstrated significantly lower numbers of CD45^{+}, F4/80^{+} cells and Ly6G^{+} cells in CL-11$^{-/-}$ kidneys at 7 post-reperfusion compared with CL-11$^{+/+}$ controls (Fig, 3c), in agreement with flow cytometry data. In addition, we assessed the effect of CL-11 on renal tissue inflammation and fibrogenesis following renal IR injury. Intrarenal gene expression of proinflammatory cytokines (TNF-α, IL-1β, IL-6), chemokines (CXCL1, CCL2) and profibrotic factors (TGF-β, PDGF) was significantly lower in CL-11$^{-/-}$ kidneys compared to CL-11$^{+/+}$ controls at 7 days post-reperfusion (Fig. 4). These results together demonstrate that CL-11 is required for renal inflammatory cell infiltration, tissue inflammation and fibrogenesis following renal IR injury.

CL-11 promotes leukocyte migration *in vitro*

The association of CL-11 with renal inflammatory cell infiltration raises the question of whether CL-11 has direct effect on leukocyte migration. It has been reported that several plant lectins such as concanavalin A (Con A) and peanut agglutinin can promote human neutrophil migration,[26] in a carbohydrate-dependent manner. We speculated that CL-11 may have such function. We therefore performed a chemotaxis assay to evaluate the effects of CL-11 on leukocyte migration using murine peritoneal exudate cells (>80% neutrophil/MO/MΦ) and recombinant CL-11 (rCL-11). We first

characterized the rCL-11 by western blot. Under a reducing condition, rCL-11 displayed a (predicted) band with 34 kDa molecular weight, reflecting a monomeric unit of CL-11. This band was also detected in normal mouse serum (sFig. 1). We also checked and confirmed that the endotoxin levels in the working concentrations of rCL-11 used in our study are far below the reported lowest concentration of endotoxin (0.5 ng/mL) that showed effects in cell culture experiments, according to the company datasheet. Our chemotaxis results showed that rCL-11strongly induced leukocyte migration in a rCL-11 dose-dependent manner (150 ng/mL-1200 ng/mL) (Fig. 5a). Migration induced by rCL-11(600 ng/mL) was comparable to that induced by *N*-formyl-met-leu-phe (fMLP), a well-described chemoattractant (100nM) (Fig. 5b), indicating the potency of CL-11 in chemotaxis. To assess the possibility that CL-11 mediates leukocyte migration through complement activation, we performed the chemotaxis assay using peritoneal exudate cells from $C3^{-/-}$ mice. Results showed that CL-11 significantly increased the migration of $C3^{-/-}$ leukocytes; the effect was comparable to that on WT leukocytes (Fig. 5c). We next explored the ligands which could be responsible for CL-11 mediated leukocyte migration. We initially examined the specificity and intensity of carbohydrate moieties in our murine leukocyte preparations by lectin-binding assay using several fluorescein labelled lectins: galanthus nivalis lectin (GNL) (for detection of terminal α (1,3) linked mannose residues), lens culinaris agglutinin (LCA) (for detection of branched fucose/α-linked mannose residues), lotus tetragonolobus (LTL) (for detection of terminal α-L-fucose and fucose alone) and ulex europaeus I (UEA I) (for detection of α(1,2) linked fucose residues). Flow cytometry analysis showed that GNL, LCA, LTL and UEA I were able to bind to murine leukocytes; markedly high binding intensities were observed with GNL and LCA, indicating predominant presence of mannosyl residues (Man) on the cell surface (sFig. 2a). We then assessed whether blocking carbohydrate recognition of CL-11 by using its preferential monosaccharide ligands (L-fucose, D-mannose) could inhibit chemotactic effect of CL-11 on leukocytes. Pre-incubation of rCL-11 with D-mannose effectively reduced CL-11 mediated leukocyte migration. Pre-incubation with L-fucose led to a small reduction of the migration, but pre-incubation with a less preferred monosaccharide ligand (D-galactose) had no effect on CL-11 mediated leukocyte migration (Fig. 5d). These results demonstrate that CL-11 has a chemotactic effect on murine leukocytes, and the effect is carbohydrate-dependent.

CL-11 stimulates renal fibroblast proliferation *in vitro*

Renal interstitial fibroblasts are the key effector cells in the development of renal fibrosis. Plant lectins such as Con A are known to have stimulatory effects on hamster renal fibroblast proliferation.[27] We therefore sought to investigate the possibility that CL-11 can stimulate renal fibroblast proliferation. To this end, we cultured primary renal fibroblasts from mice and confirmed that >95% were positive

for vimentin (sFig. 3). Proliferation assay was performed on the fibroblasts treated with rCL-11 and controls for 24h using Click-iT® EdU Alexa Fluor® 488 Imaging Kit. Initial experiments showed that treatment of fibroblasts with different concentrations of rCL-11 (in the range of 300-1200 ng/mL) significantly increased EdU-labelled cell numbers, with a maximal stimulation at 600 ng/mL (Fig. 6a). The stimulatory effect of CL-11 on fibroblast proliferation was further confirmed at the concentration of 600 ng/mL, which is comparable to that stimulated by Con A at 1 μg/mL concentration (Fig. 6b, 6c). These results clearly demonstrate that CL-11 has stimulatory effects on renal fibroblasts.

It has been shown that CL-11 preferentially binds to mannose-containing glycans.[18] We therefore sought to investigate whether the effect of CL-11 on renal fibroblast proliferation is dependent on interaction with Man on renal fibroblast surface. We first examined the specificity and intensity of carbohydrate moieties on renal fibroblasts by using fluorescein labelled lectins. Flow cytometry revealed the high binding intensities of GNL and LCA and the low binding intensities of UEA-I and LTL, indicating predominant presence of Man on renal fibroblast surface (sFig. 2b). Fluorescence microscopy confirmed this by showing positive staining of GNL and LCA in renal fibroblasts (Fig. 6d). Using confocal microscopy, presence of Man on the cell surface also corresponded with CL-11 binding (Fig. 6e). We then assessed whether blocking CL-11-Man interaction can inhibit the effect of CL-11 on renal fibroblast proliferation. Proliferation assay showed that prior treatment of renal fibroblasts with α-mannosidase significantly inhibited CL-11 mediated fibroblast proliferation, when compared with control treatment; but prior treatment with β-galactosidase did not affect CL-11 mediated fibroblast proliferation (Fig. 6f). These observations support the concept that Man on the surface of renal fibroblasts is involved in CL-11-mediated fibroblast proliferation.

Local production of CL-11 in the kidney plays an important role in the development of renal tubulointerstitial fibrosis

CL-11 has relatively low serum concentrations (~300 ng/mL), compared to MBL (~2 μg/mL), and usually exists in the circulation as a dimeric or trimeric form (>200kD). When complexed with CL-10 in the circulation, it forms a large molecule (up to 800kD). These large molecules may not be able to penetrate into the interstitial space of organs including the kidney. Therefore, we hypothesized that local production of CL-11 within the kidney is important for the development of renal tubulointerstitial fibrosis. To test this, we performed syngeneic mouse kidney transplantation in the following combinations: i) CL-11$^{-/-}$ (donor) to CL-11$^{+/+}$ (recipient), ii) CL-11$^{+/+}$ (donor) to CL-11$^{+/+}$ (recipient) and assessed donor renal tubular damage (by PAS staining) and collagen deposition (by Sirius red staining) at 7 days post-transplantation. CL-11$^{-/-}$ isografts displayed much less tubular damage and

collagen deposition than CL-11$^{+/+}$ controls (Fig. 7). The extent of reduction in tubular damage and collagen deposition in CL-11$^{-/-}$ isografts was comparable to that observed in the kidneys of CL-11$^{-/-}$ mice (have a generalized CL-11 deficiency) following renal IR injury, indicating a predominant role for local production of CL-11 in this model.

Discussion

Our recent work in a murine model of acute renal IR injury has shown that AKI in the early phase is dependent on CL-11.[21] It was proposed that CL-11 detects stress-induced L-fucose pattern on renal tubules to trigger complement activation that mediates renal tubular epithelial injury. In the present study, we extended our observations to the late phase of renal IR injury and examined the impact of CL-11 on renal chronic inflammation and fibrosis following renal IR. Overall, our data clearly demonstrate a pathogenic role for CL-11 in the progression of renal tubulointerstitial fibrosis, and suggest novel mechanisms for the pro-fibrotic effects of CL-11, namely the promotion of leukocyte migration and stimulation of renal fibroblast proliferation.

A key observation from this study is that renal chronic inflammation and tubulointerstitial fibrosis are dependent on CL-11. We have shown that CL-11$^{-/-}$ mice are protected from deterioration of renal function, with attenuated renal chronic tissue inflammation (i.e. inflammatory cell infiltration, tubule injury, intrarenal synthesis of pro-inflammatory and pro-fibrotic molecules) and attenuated ECM accumulation in the tubulointerstitial space. In renal isografts, attenuated tubule damage and collagen deposition were only observed in CL-11-deificient kidneys. This observation gives rise to an intriguing question of how CL-11 contributes to chronic renal inflammation and tubulointerstitial fibrosis.

In terms of the cellular mechanisms underlying this novel pathogenic role of CL-11 as a mediator of chronic renal inflammation and tubulointerstitial fibrosis, we have made two important *in vitro* observations. First, a potent effect of CL-11 on leukocyte (mainly neutrophil/MO/MΦ) migration was observed, indicating that CL-11 has chemotactic activity. Given that our leukocyte migration assays were performed in a serum-free condition and CL-11 had clear effects on leukocyte migration, in the absence of complement activation, the effect of CL-11 on leukocyte migration is likely to be complement-independent, thus suggesting CL-11 has a direct, complement-independent effect on leukocyte migration, which is consistent with reported roles for plant lectins in neutrophil migration [26] and more recently for CL-11 in HeLa cell migration.[19] In support of this complement-independent effect, our *in vivo* observations showed that although renal cellular infiltration was persistently lower in CL-11$^{-/-}$ mice than that in CL-11$^{+/+}$ mice at day 2 and day 7 post-reperfusion, complement activation in the

kidneys as measured by C3d deposition was not a prominent feature in the late phase of injury, which was also comparable between the WT and CL-11$^{-/-}$ mice (sFig. 4). Therefore, in addition to the proinflammatory action of CL-11 on tubular epithelial cells in the early phase of IR injury which triggers inflammatory responses (i.e. complement activation, cellular infiltration) to cause tubular injury, CL-11 released from stressed or damaged tubular epithelial cells (or other cells) may function as a chemoattractant for leukocytes, promoting inflammatory cell infiltration, thereby exacerbating renal tissue inflammation and driving the profibrotic process. Secondly, renal fibroblast proliferation, a key cellular process directing renal fibrosis, was significantly enhanced by CL-11 stimulation, demonstrating an important role for CL-11 in renal fibroblast proliferation. Fibroblasts (e.g. from skin, synovial) are a known source of complement[28, 29] and it is possible that binding of CL-11 may cause the cell activation via complement activation. However, CL-11-mediated complement activation does not appear to be prominent in our fibroblast culture system (sFig. 5), as there is no indication of complement deposition on renal fibroblasts following CL-11 stimulation, although the possibility of a complement-dependent effect *in vivo* cannot be excluded. Therefore, locally produced CL-11 may function as stimulator for renal fibroblast, promoting cell proliferation, thus contributing to the progression of tubulointerstitial fibrosis.

Our observation on CL-11 promoting leukocyte migration and renal fibroblast proliferation *in vitro* raised the question of which ligands responsible for CL-11 mediating these cellular processes. L-fucose, mannose and mannose-containing glycans have been suggested as preferential binding ligands for CL-11[17, 18]. In our previous study in acute renal IR injury, we proposed that CL-11 recognizes stress associated L-fucose pattern on proximal tubular epithelial cells upon ischemic insult. This is based on the fact that L-fucose is exclusively and abundantly produced by proximal tubular epithelial cells and is a maker for this type of cells in the kidney, and our observation that a disorganized pattern of L-fucose was expressed and aligned with CL-11 in the basolateral border of the proximal tubules in ischemic kidneys. In this study, the flow cytometry and fluorescence microscopy confirm that Man are predominantly present on the cell surface of leukocytes and renal fibroblasts. With regard to the molecule(s) responsible for the action of CL-11 on leukocyte migration, our blocking experiments showed that pre-incubation of rCL-11 with D-mannose or L-fucose was able to block the effect of CL-11-mediated leukocyte migration, indicating the action is carbohydrate-dependent. In support of this, previous studies have shown that neutrophil chemotaxis mediated by several plant lectins was effectively inhibited by pre-incubation of the lectins with their carbohydrate ligands.[26] Furthermore, our lectin screening results revealed predominant expression of Man on leukocyte cell surface supporting that CL-11-mediated leukocyte migration is mainly through a Man recognition mechanism. With regard to the molecule(s) responsible for the action of CL-11 on renal

fibroblast proliferation, our study suggests that Man is also involved in CL-11-mediated cell proliferation. This is supported by our findings that CL-11 binds to Man on the fibroblast cell surface and removal of mannose (using α-mannosidase), but not galactose (using β-galactosidase) abrogates the effects of CL-11 on the fibroblast proliferation.

Predominant presence of Man on the cell surface of leukocytes and renal fibroblasts raises possibility of that other collectins (e.g. MBL, SP-A) could play similar roles as CL-11 in these cellular processes, thus participating in the pathogenesis of renal fibrosis

Renal inflammation is an initial protective response to kidney injury. However, excessive inflammatory responses in the kidney upon injury or unresolved renal inflammation are thought to be an important driver of the process of the fibrosis.[9] This notion is further supported by our *in vitro* observations that supernatants, resulting from co-cultures of inflammatory cells (murine peritoneal exudate cells) with tubular debris, contained high levels of pro-inflammatory cytokines (TNF-α, IL-1β, and TGF-β) and were able to stimulate renal fibroblast proliferation (sFig. 6). Therefore, CL-11-mediated acute kidney injury (tubule damage, cellular infiltration), as a consequence of complement activation, would also stimulate the process of tubulointerstitial fibrosis. In agreement with this, $C3^{-/-}$ mice which have intact CL-11 also displayed less collagen deposition in the peritubular interstitium and cellular infiltration in the kidney on day 7 post-reperfusion (sFig. 7). Thus, there is a possibility that collectin-11 may be causing fibrosis *in vivo*, at least partly, through the earlier activation of complement.

Based on our findings in this study and our published data in the study of acute injury,[21] we propose that CL-11 contributes to chronic renal inflammation and tubulointerstitial fibrosis through three pathways: namely i) by stimulating renal fibroblast proliferation, ii) by mediating influx of inflammatory cells, iii) by triggering complement activation that increases renal tissue inflammation and fibrogenesis (Fig. 8).

In conclusion, this study is the first to demonstrate a pathogenic role for CL-11 in the development of kidney fibrosis, and describes novel cellular and molecular mechanisms for CL-11 that contribute to progression of tubulointerstitial fibrosis, thus opening new avenues for studying the roles of CL-11 in renal fibrosis mediated by other causes and supporting therapeutic blocking the CL-11-ligand interaction in tubulointerstitial fibrosis.

Materials and Methods

Reagents

The following reagents were used in the current study: Infinity Urea (655870, Fisher Diagnosis, Virginia, USA); rat monoclonal anti-F4/80 Ab (ab16911), rabbit polyclonal anti-collagen 1 Ab (ab34710), rabbit polyclonal anti-fibronectin Ab (ab2413), rabbit monoclonal anti-vimentin Ab (EPR3776) (ab92547) (all are from Abcam, Cambridge, UK); TRITC-conjugated goat anti-rabbit IgG Ab (T6778, Sigma, Missouri, USA); rat monoclonal anti-CD45 Ab (MCD4500; Caltag Laboratories, California, USA); rat monoclonal anti-Ly-6B.2 Ab (MCA771G, Bio-Rad antibodies, Oxfordshire, UK); HRP-conjugated rabbit anti-rat Ig Ab (P0450; DAKO); APC rat anti-mouse CD45 Ab (103112), PE rat anti-mouse Ly-6G Ab (127607), FITC rat anti-mouse F4/80 Ab (123108) and PE/Cy7 rat anti-mouse Ly-6C Ab (128018) (all are from Biolegend, London, UK); Rabbit polyclonal anti-human C3d Ab (A0063; DAKO, Glostrup, Denmark); FITC-conjugated goat anti-rabbit IgG Ab (111-095-144; Jackson Immuno Research Lab., West Grove, USA); rabbit polyclonal anti-human CL-11 (abx003772; Abbexa Ltd, Cambridge, UK); donkey anti-rabbit Alexa Fluor 594 (406418; Biolegend, London, UK); 4',6-diamidino-2-phenylindole (DAPI), Alexa 488 phalloidin (A12379), CountBright™ absolute counting beads (C36950) (all are from Life Technologies, Paisley, UK); recombinant CL-11 (rCL-11, C7549-85; USBiological, Massachusetts, USA); Fluorescein labelled Ulex Europaeus I (UEA-I) (FL-1061), Fluorescein labelled Lotus Tetragonolobus Lectin (LTL) (FL 1321), Fluorescein labelled Lens Culinaris Agglutinin (LCA) (FL-1041), Fluorescein labelled Galanthus Nivalis Lectin (GNL) (FL-1241),(all are from Vector laboratories, Peterborough, UK); D-(+)-Mannose (M6020), L-(-)-Fucose (F2262), D-(+)-Galactose (G0750), α-mannosidase (M7257), β-glactosidase (G5635) (all are from Sigma, Missouri, USA); Mouse TNFα (555268) and IL-1β (559603) ELISA sets (BD Bioscience, San Jose, USA); Click-iT® EdU Alexa Fluor® 488 Imaging kit (C10337; Thermo Fisher Scientific, Paisley, UK); Thioglycollate (CM0023, Oxoid, Hampshire, UK); collagenase II (LS004176, Worthington on Biochemical corporation, USA).

Mice

Homozygous CL-11$^{-/-}$ mice on a C57BL/6 background were purchased from Mutant Mouse Resource and Research Centers (MMRRC) (UC Davis, Davis California, USA) [30] and have been back crossed onto the C57BL/6 strain for 6 generations . WT littermates (CL-11$^{+/+}$) were used as controls. Male mice (8-12 weeks) were used in all the experiments, unless specified. Animal procedures adhered to the Animals (Scientific Procedures) Act of 1986.

Induction of renal IR injury

Renal IR injury was induced as we previously described with some modifications. [31] In brief, mice were anesthetized by isoflurane and kept warm on a heated pad. A midline abdominal incision was made. The renal arteries and veins were isolated and bilaterally occluded for 30 min with micro aneurysm clamps. After removal of the clamps, 0.5 ml of warm saline was put in the abdomen and the incision was sutured. Blood samples were taken at day 2 (tail bleeding) and day 7 (cardiac puncture) after reperfusion for renal function assessment. Kidneys were harvested at day 7 for histopathology, flow cytometry and RT-qPCR.

Assessment of renal function, pathology and fibrosis

Renal function was assessed by measuring the blood urea nitrogen (BUN) in the serum using a standard urease kit called Infinity Urea. Renal histopathological changes and fibrosis were assessed as described previously.[32] In brief, kidneys were fixed with 4% formaldehyde in PBS for 48 hours and embedded in paraffin. Paraffin sections (2~4 μm) were stained with periodic acid-Schiff (PAS) stain, or Sirius red. Stained kidney sections were scanned with a Hamamatsu Nanozoomer 2.0 HT slide scanner (Hamamatsu Photonics, Hamamtsu, Japan) and viewed using NDP.view2 software. Renal histopathological changes were assessed on PAS–stained sections using a 6-point scale in which 0, 1, 2, 3, 4, and 5 indicated normal, very little, very mild, mild, moderate, and severe histological lesions, respectively, as previous description.[32] The assessment was based on histopathological changes (i.e. cellular infiltration, loss of proximal tubule brush border, tubule necrosis, tubule atrophy) that were mainly located at the cortical medullary junction area. Five viewing fields (0.49 mm^2/field) from each kidney were examined. Renal fibrosis was assessed on Sirius red–stained sections. The positively stained areas were quantified by imaging analysis (ImageJ software; National Institutes of Health, Bethesda, MD, USA). Briefly, 6 to 8 viewing fields from the cortical medullary junction of each kidney were examined. Positively stained areas were expressed as a percentage of the whole field area (0.49 mm^2). All the aforementioned quantitative analyses were performed in a blinded fashion by 2 experienced persons.

Immunohistochemistry

Immunohistochemistry was performed on frozen sections (~4 μm) of kidneys. For the detection of inflammatory cells, kidney sections were fixed in acetone and blocked by 10% rabbit serum, then incubated with rat anti-mouse CD45, Ly-6B.2, and F4/80 antibodies, respectively, at 4°C overnight and followed by HRP-conjugated rabbit anti-rat polyclonal antibody. The sections were scanned with a Hamamatsu Nanozoomer 2.0 HT slide scanner. Four fields (0.12 mm^2 per field) in the cortical medullary junction of each kidney were randomly examined and the positively stained cells were

counted. The quantitative analysis was performed in a blinded fashion by two experienced persons. For the detection of extracellular matrix deposition, kidney sections were incubated overnight at 4°C with donkey anti-mouse collagen 1, fibronectin, and vimentin, respectively, and followed by TRITC-conjugated goat anti-rabbit IgG Ab, DAPI (staining nuclei) and LTL (staining proximal tubules). The staining was examined via an A1R point scanning confocal microscope (Nikon, Japan) or an Olympus BX51 microscope (Japan).

Assessment of inflammatory cell infiltration in the kidney

Single renal cell suspensions were prepared using a method described previously.[32] Kidneys were weighed, minced and incubated with collagenase D (0.75 mg/mL) for 10 min at 37°C with gentle agitation. The collagenase was inactivated with an equal volume of DMEM-F12 containing 10% FCS. The digested tissue mixture was then passed through a 40μm nylon sieve to remove tissue debris. The cell segments were collected and treated with red cell lysis buffer to remove remaining RBC. The cell pellet was washed and re-suspended in PBS containing 1% BSA and followed by flow cytometric analysis. The cells were pre-incubated with FcR blocking antibody (CD16/32), and then stained with rat anti-mouse APC-conjugated CD45, PE-conjugated Ly6G and FITC-conjugated F4/80 antibodies, or the appropriate isotype control antibodies at 4°C for 20 min. In order to quantify absolute cell counts in kidney tissue, we used CountBright™ absolute counting beads in our flow cytometry assays, according to the manufacturer's instructions. All flow cytometric analysis was performed using Calibur Flow Cytometer (BD Biosciences) and Flowjo software (Tree Star, OR, USA).

Reverse Transcription Quantitative PCR (RT-qPCR)

Total RNA extraction from kidney tissue and cells and reverse transcription reaction were performed as previously described.[33] qPCR was performed with a DyNAmo HS SYBR Green qPCR kit and an MJ Research PTC-200 Peltier Thermal Cycler (Bio-Rad) according to the manufactures' instructions. Each sample was amplified in duplicates. The relative gene expression was analyzed using the $2^{-\Delta\Delta CT}$ method [34] and expressed as $2^{-\Delta\Delta\ (Ct)}$, where Ct is cycle threshold, ΔΔ (Ct) = testing samples Δ (Ct) - control samples Δ (Ct); Δ (Ct) = testing gene (Ct) -18s (Ct). The control samples were normal CL-$11^{+/+}$ kidneys and the testing samples were injured kidneys. The primer sequences and size are shown in the supplemental table 1.

Chemotaxis assay

Chemotaxis assay was performed with murine peritoneal exudate cells (>80% neutrophil/MO/MΦ) which were prepared from peritoneal lavage of $C3^{-/-}$ or CL-11 WT mice 1 day after i.p. injection of 1 mL of 3% thioglycollate using a disposable 96-well cell migration system (106-3; Neuro Prob). 30 μl of cell

culture medium (RPMI 1640 with1% BSA) (negative control) or the medium containing rCL-11 (150-1200ng/mL) or fMLP (100 nM) (positive control) were added to each chamber well. The framed filters with 3 μm pore size were placed to chamber wells and 50 μL of cell suspension ($2x10^5$ cells in RPMI 1640 with1% BSA) were add to the top of each filter. The chamber was incubated for 1.5 hours at 37°C with 5% CO_2. The cells migrated to the bottom of each well were collected and stained with trypan blue and counted under microscope. In some experiments, rCL-11 (600 ng/mL) was pre-incubated with 2.5 mM of D-mannose, L-fucose or D-galactose for 1 hour at room temperature in the presence of 2 mM Ca^{2+} and then added to the lower chamber wells.

Mouse renal fibroblast culture

Primary renal fibroblast culture was prepared from kidneys of CL-$11^{+/+}$ mice as described previously with some modifications.[35] In brief, the renal capsule was peeled off and a longitudinal incision was made on the kidney. The sections of cortex were carefully cut off and diced into mince. They were digested with 0.1% collagenase II in DMEM/F-12 medium for 20 min and passed through 250 μm, 106 μm, and 75 μm metal sieves and a 40 μm nylon sieve. The unfiltered tubular debris on the nylon sieve was collected and treated macrophages for the study of cytokine expression described below. The filtered cells were cultured in DMEM/F-12 medium containing 10% FCS and 100 U/ml penicillin and 100 μg/ml streptomycin. They experienced at least three passages to eliminate contaminated epithelial cells. Finally, the pure fibroblasts exhibited an elongated, spindle-shaped morphology with vimentin positive staining in immunohistochemistry.

Proliferation assay

Mouse renal fibroblasts were seeded on 1% gelatin-coated 8 mm cover glass in a 48-well plate with $3x10^4$ cells per well. They came to 70-80% confluence after 2 days of culture. The cells were incubated in the medium only (DMEM/F-12 with 5% FCS) or the medium containing different concentrations of rCL-11 (300-1200 ng/mL) or Con A (1 μg/mL) for 24 h. In some experiments, cells were pre-incubated with or without 5 mM α-mannosidase or β-galactosidase diluted in glycol buffer 3 and DMEM/F-12 for 1 hour at 37°C. After three washes in PBS, the cells were continued to treat with 600 ng/mL rCL-11 for 24 h. At the end of rCL-11 treatment, cells were incubated with serum-free DEME/F-12 containing 10 mM EdU for 2 h and fixed in 3.7% formaldehyde. Incorporated EdU was detected by a Click-iT® EdU Alexa Fluor® 488 Imaging kit according to manufacturer's instructions. Pictures were taken by an Olympus BX51 microscope. The DAPI-positive nuclear (representing the total cell number) and EdU positive nuclear (representing the proliferating cell number) were counted using Image J. The proliferation rate was calculated using the following formula: proliferation rate = (EdU positive nuclear number/DAPI positive nuclear number) x 100%.

Detection of mannosyl residues in renal fibroblasts

The mouse renal fibroblasts were fixed in 4% PFA for 15 min (without permeablization) and stained with DAPI and fluorescein-labelled GNL and LCA for 1 hour at room temperature. Pictures were taken with an A1R point scanning confocal microscope.

Detection of CL-11 binding to renal fibroblasts

the renal fibroblasts cultured from CL-11$^{-/-}$ mice were incubated with rCL-11 (600 ng/mL) for 24 h and fixed in 4% PFA for 15 min. Without cell membrane permeablization, the cells were blocked with 10% donkey serum and incubated with rabbit anti-human CL-11 antibody overnight at 4°C, followed by the secondary donkey anti-rabbit Alexa Fluor 594 antibody, fluorescein-labelled GNL or LCA and DAPI for 1 hour at room temperature. The staining was examined via an A1R point scanning confocal microscope.

Mouse kidney transplantation

Kidney transplants were performed in mice as previously described.[21] Briefly, mice were anesthetized with isoflurane (Abbott Laboratories). Donor kidney along with the ureter was harvested, including the renal artery with a small aortic cuff and the renal vein. These vascular cuffs were anastomosed to the recipient abdominal aorta and vena cava, respectively, below the level of the native renal vessels. Total ischemic time was about 35 min. The donor ureter was connected to the recipient bladder. The right native kidney was removed before the vascular anastomosis. The transplanted kidney was collected 7 days after surgery. PAS and Sirius red staining were performed to assess tissue damage and renal fibrosis.

Statistics

Data are shown either as mean ± SEM or the readout for individual mice. An unpaired, 2-tailed Student's t test was used to compare two groups. A *P* value less than 0.05 was considered significant. One-way ANOVA was used for comparisons between three or more groups. All analyses were performed using Graph Pad Prism Version 5 (Graph Pad Software).

Conflict of interest

The authors would like to declare that no conflict of interest exists

Acknowledgements

This work was supported by the Medical Research Council of the UK (MR/L020254/1 to WZ and SS) (MR/J006742/1 to SS and WZ), the National Natural Science Foundation of China (NSFC 81170644 to KL) and the Visiting Scholarship of Xi'an Jiaotong University to KCL.

References

[1] Jha V, Garcia-Garcia G, Iseki K, Li Z, Naicker S, Plattner B, Saran R, Wang AY, Yang CW: Chronic kidney disease: global dimension and perspectives. Lancet (London, England) 2013, 382:260-72.
[2] Venkatachalam MA, Griffin KA, Lan R, Geng H, Saikumar P, Bidani AK: Acute kidney injury: a springboard for progression in chronic kidney disease. American journal of physiology Renal physiology 2010, 298:F1078-94.
[3] Zeisberg M, Neilson EG: Mechanisms of tubulointerstitial fibrosis. Journal of the American Society of Nephrology : JASN 2010, 21:1819-34.
[4] Liu Y: Cellular and molecular mechanisms of renal fibrosis. Nature reviews Nephrology 2011, 7:684-96.
[5] Duffield JS: Cellular and molecular mechanisms in kidney fibrosis. The Journal of clinical investigation 2014, 124:2299-306.
[6] Eddy AA: The origin of scar-forming kidney myofibroblasts. Nature medicine 2013, 19:964-6.
[7] Meran S, Steadman R: Fibroblasts and myofibroblasts in renal fibrosis. International journal of experimental pathology 2011, 92:158-67.
[8] LeBleu VS, Taduri G, O'Connell J, Teng Y, Cooke VG, Woda C, Sugimoto H, Kalluri R: Origin and function of myofibroblasts in kidney fibrosis. Nature medicine 2013, 19:1047-53.
[9] Meng XM, Nikolic-Paterson DJ, Lan HY: Inflammatory processes in renal fibrosis. Nature reviews Nephrology 2014, 10:493-503.
[10] Holmskov U, Thiel S, Jensenius JC: Collections and ficolins: humoral lectins of the innate immune defense. Annual review of immunology 2003, 21:547-78.
[11] Weis WI, Drickamer K, Hendrickson WA: Structure of a C-type mannose-binding protein complexed with an oligosaccharide. Nature 1992, 360:127-34.
[12] Schwaeble W, Dahl MR, Thiel S, Stover C, Jensenius JC: The mannan-binding lectin-associated serine proteases (MASPs) and MAp19: four components of the lectin pathway activation complex encoded by two genes. Immunobiology 2002, 205:455-66.
[13] Kuhlman M, Joiner K, Ezekowitz RA: The human mannose-binding protein functions as an opsonin. The Journal of experimental medicine 1989, 169:1733-45.
[14] Ofek I, Mesika A, Kalina M, Keisari Y, Podschun R, Sahly H, Chang D, McGregor D, Crouch E: Surfactant protein D enhances phagocytosis and killing of unencapsulated phase variants of Klebsiella pneumoniae. Infection and immunity 2001, 69:24-33.
[15] Henriksen ML, Brandt J, Iyer SS, Thielens NM, Hansen S: Characterization of the interaction between collectin 11 (CL-11, CL-K1) and nucleic acids. Molecular immunology 2013, 56:757-67.
[16] Ma YJ, Skjoedt MO, Garred P: Collectin-11/MASP complex formation triggers activation of the lectin complement pathway--the fifth lectin pathway initiation complex. Journal of innate immunity 2013, 5:242-50.
[17] Selman L, Hansen S: Structure and function of collectin liver 1 (CL-L1) and collectin 11 (CL-11, CL-K1). Immunobiology 2012, 217:851-63.
[18] Venkatraman Girija U, Furze CM, Gingras AR, Yoshizaki T, Ohtani K, Marshall JE, Wallis AK, Schwaeble WJ, El-Mezgueldi M, Mitchell DA, Moody PC, Wakamiya N, Wallis R: Molecular basis of sugar recognition by collectin-K1 and the effects of mutations associated with 3MC syndrome. BMC biology 2015, 13:27.
[19] Rooryck C, Diaz-Font A, Osborn DP, Chabchoub E, Hernandez-Hernandez V, Shamseldin H, Kenny J, Waters A, Jenkins D, Kaissi AA, Leal GF, Dallapiccola B, Carnevale F, Bitner-Glindzicz M, Lees M, Hennekam R, Stanier P,

Burns AJ, Peeters H, Alkuraya FS, Beales PL: Mutations in lectin complement pathway genes COLEC11 and MASP1 cause 3MC syndrome. Nature genetics 2011, 43:197-203.
[20] Hwang I, Mori K, Ohtani K, Matsuda Y, Roy N, Kim Y, Suzuki Y, Wakamiya N: Collectin Kidney 1 Plays an Important Role in Innate Immunity against Streptococcus pneumoniae Infection. Journal of innate immunity 2017, 9:217-28.
[21] Farrar CA, Tran D, Li K, Wu W, Peng Q, Schwaeble W, Zhou W, Sacks SH: Collectin-11 detects stress-induced L-fucose pattern to trigger renal epithelial injury. The Journal of clinical investigation 2016, 126:1911-25.
[22] Kawakami T, Ren S, Duffield JS: Wnt signalling in kidney diseases: dual roles in renal injury and repair. The Journal of pathology 2013, 229:221-31.
[23] Kramann R: Hedgehog Gli signalling in kidney fibrosis. Nephrology, dialysis, transplantation : official publication of the European Dialysis and Transplant Association - European Renal Association 2016, 31:1989-95.
[24] Church RH, Ali I, Tate M, Lavin D, Krishnakumar A, Kok HM, Goldschmeding R, Martin F, Brazil D: Gremlin1 plays a key role in kidney development and renal fibrosis. American journal of physiology Renal physiology 2017:ajprenal.00344.2016.
[25] Shi W, Xu J, Warburton D: Development, repair and fibrosis: what is common and why it matters. Respirology (Carlton, Vic) 2009, 14:656-65.
[26] Kuehn C, Van Epps DE: Lectin-mediated induction of human neutrophil chemotaxis, chemokinesis, and cap formation. Infection and immunity 1980, 29:600-8.
[27] Aubery M, Bourrillon R, O'Neill C H: Stimulation of the proliferation of normal BHK21 cultured fibroblasts by plant lectins. Experimental cell research 1975, 93:47-54.
[28] Katz Y, Revel M, Strunk RC: Interleukin 6 stimulates synthesis of complement proteins factor B and C3 in human skin fibroblasts. European journal of immunology 1989, 19:983-8.
[29] Katz Y, Strunk RC: Synovial fibroblast-like cells synthesize seven proteins of the complement system. Arthritis and rheumatism 1988, 31:1365-70.
[30] Tang T, Li L, Tang J, Li Y, Lin WY, Martin F, Grant D, Solloway M, Parker L, Ye W, Forrest W, Ghilardi N, Oravecz T, Platt KA, Rice DS, Hansen GM, Abuin A, Eberhart DE, Godowski P, Holt KH, Peterson A, Zambrowicz BP, de Sauvage FJ: A mouse knockout library for secreted and transmembrane proteins. Nature biotechnology 2010, 28:749-55.
[31] Zhou W, Farrar CA, Abe K, Pratt JR, Marsh JE, Wang Y, Stahl GL, Sacks SH: Predominant role for C5b-9 in renal ischemia/reperfusion injury. The Journal of clinical investigation 2000, 105:1363-71.
[32] Choudhry N, Li K, Zhang T, Wu KY, Song Y, Farrar CA, Wang N, Liu CF, Peng Q, Wu W, Sacks SH, Zhou W: The complement factor 5a receptor 1 has a pathogenic role in chronic inflammation and renal fibrosis in a murine model of chronic pyelonephritis. Kidney international 2016, 90:540-54.
[33] Hong Y, Zhou W, Li K, Sacks SH: Triptolide is a potent suppressant of C3, CD40 and B7h expression in activated human proximal tubular epithelial cells. Kidney international 2002, 62:1291-300.
[34] Livak KJ, Schmittgen TD: Analysis of relative gene expression data using real-time quantitative PCR and the 2(-Delta Delta C(T)) Method. Methods (San Diego, Calif) 2001, 25:402-8.
[35] Springall T, Sheerin NS, Abe K, Holers VM, Wan H, Sacks SH: Epithelial secretion of C3 promotes colonization of the upper urinary tract by Escherichia coli. Nature medicine 2001, 7:801-6.

Figure legends

Figure 1. Deficiency of CL-11 reduces tubule damage and renal function impairment in the late phase of renal IR. (**a**) BUN levels in CL-$11^{+/+}$ and CL-$11^{-/-}$ mice at day 2 and day 7 post renal ischemia (30 min) reperfusion. Data were analysed by two-way ANOVA. Dashed line represents the BUN level in normal mice. (**b**) Representative images of PAS staining on kidneys of CL-$11^{+/+}$ and CL-$11^{-/-}$ mice at day 7 post renal ischemia reperfusion, taken at the cortical-medullary junction. Arrows indicate injured tubules. Scale bars: 100 μm. (**c**) Histological scores for renal tubular injury in the mice illustrated in b. Data were analysed by Unpaired two-tailed Student's *t* test. ****, *P*<0.0001. (**a, c**): each dot represents an individual mouse and a representative of two independent experiments is shown.

Figure 2. Deficiency of CL-11 reduces accumulation of ECM in the kidney following renal IR. (**a**) Representative images of Sirius red staining on kidneys of CL-$11^{+/+}$ and CL-$11^{-/-}$ mice at day 7 post renal ischemia reperfusion, taken at the cortical-medullary junction. Scale bars: 100 μm. Arrows indicate positive stained arears. (**b**) Quantification of Sirius red stained arears corresponding to the CL-$11^{+/+}$ and CL-$11^{-/-}$ mice in a. Data were analysed by Unpaired two-tailed Student's *t* test (n=35-50 viewing fields from 7-9 mice/group), ***, *P*<0.0001. (**c**) Extracellular matrix protein (ECM) deposition in kidneys. Left panels, representative fluorescence microscope images of collagen I (red), fibronectin (red), vimentin (red), lotus tetragonolobus lectin (LTL) (a proximal tubular marker) (green), DAPI (blue) staining on kidneys of CL-$11^{+/+}$ and CL-$11^{-/-}$ mice at day 7 post renal ischemia reperfusion, taken at the cortical-medullary junction. Arrows indicate positive stained arears. Scale bars: 20 μm. Right panels, quantification of positively stained arears of collagen I, fibronectin and vimentin, corresponding to the CL-$11^{+/+}$ and CL-$11^{-/-}$ mice in left panels. Data were analysed by Unpaired two-tailed Student's *t* test (n=6 viewing fields from 2 mice/group). ***, *P*<0.001. (**d**) Relative mRNA levels of collagen I (Col I) and fibronectin (FN) in kidneys of CL-$11^{+/+}$ and CL-$11^{-/-}$ mice at day 7 post renal ischemia reperfusion, determined by RT-qPCR. Data were analysed by Unpaired two-tailed Student's *t* test (n=6-7 mice per group). Each dot represents an individual mouse. *, *P*<0.05; **, *P*<0.01.

Figure 3. Deficiency of CL-11 reduces renal leukocyte infiltration following renal IR. (a, b) Renal inflammatory cell infiltration in CL-$11^{+/+}$ and CL-$11^{-/-}$ mice at day 2 and day 7 post renal ischemia reperfusion, determined by flow cytometry. (**a**) Stepwise gating strategy used in flow cytometric analysis leukocytes ($CD45^+$), neutrophils ($Ly6G^+$) and macrophages ($F4/80^+$). (**b**) Quantification of leukocytes ($CD45^+$), neutrophils ($CD45^+Ly6G^+$) and macrophages ($CD45^+F4/80^+$). Data were analysed by Unpaired two-tailed Student's *t* test (n=4 mice per group). *, *P*<0.05; **, *P*<0.01. Each dot represents an individual mouse. (**c**) Renal inflammatory cell infiltration in CL-$11^{+/+}$ and CL-$11^{-/-}$ mice at day 7 post renal ischemia reperfusion, determined by immunohistochemistry. Left panels: representative images of immunochemical staining for CD45, Ly6G and F4/80 in kidneys of CL-$11^{+/+}$

and CL-11$^{-/-}$ mice. Scale bars: 50 μm. Right panels: quantifications of CD45^{+}, Ly6G^{+} and F4/80^{+} cells in kidneys of CL-11$^{+/+}$ and CL-11$^{-/-}$ mice. Data are shown as mean ± SEM (n=31-45 viewing fields from 7-9 mice/group) and were analysed by Unpaired two-tailed Student's *t* test ***, *P*<0.0001. (**a-c**) A representative of two independent experiments is shown.

Figure 4. Deficiency of CL-11 reduces renal tissue inflammation and fibrogenesis following renal IR. Relative mRNA levels of pro-inflammatory (**a**) and pro-fibrogenic factors (**b**) in the injured kidneys of CL-11$^{+/+}$ and CL-11$^{-/-}$ mice at day 7 post renal ischemia reperfusion, determined by RT-qPCR. Data were analyzed by Unpaired two-tailed Student's *t* test, except for the PDGF that was analysed by Mann Whitney test (n=8 mice/group). Each dot represents an individual mouse. *, *P*<0.05; ***, *P*<0.001.

Figure 5. CL-11 promotes leukocyte migration *in vitro*. (**a**) Cell migration in response to medium (Ctrl), medium containing different concentrations of recombinant CL-11 (rCL-11). (**b**) Cell migration in response to medium (Ctrl), medium containing rCL-11 (600 ng/ml) or *N*-formyl-met-leu-phe (fMLP) (100 nM). (**a**, **b**) Data were analysed by One-way ANOVA with Tukey's post-test (n=5 per group). (**c**) Cell migration in response to medium (Ctrl) and medium containing rCL-11 (600 ng/ml) in C3 KO and CL-11 WT leukocytes. (**d**) Cell migration in response to rCL-11 (600 ng/ml) (rCL-11) or rCL-11 (600 ng/ml) that had been pre-incubated with D-(+)-mannose (Man), L-(-)-fucose (Fuc) or D-(+)-galactose (Gal) (all at 2.5mM). (**c**, **d**) Data were analysed by One-way ANOVA with Tukey's post-test (n=5-19). (**a**-**d**) representative of at least 3 independent experiments. *, *P*<0.05. **, *P*<0.005. ***, *P*<0.001.

Figure 6. CL-11 stimulates renal fibroblast proliferation and ECM production. (**a**) Proliferation rate of renal fibroblasts without or with different concentrations of CL-11. Data were analyzed by One-way ANOVA (n=6 viewing fields from 2 cell samples/group). ****P*<0.0001. (**b**) Representative fluorescent images of EdU-labelled renal fibroblasts without or with rCL-11 (600 ng/ml) and Concanavalin A (Con A, 1 μg/ml) treatment. Scale bars: 50 μm. (**c**) Quantification of EdU-labelled renal fibroblasts, corresponding to the fibroblasts in **b** and expressed as proliferation rate. Data were analysed by One-way ANOVA with Tukey's post-test (n=**8** viewing fields from **2** cover glass/group). **P*<0.05. ***P*<0.005. (**b, c**) A representative of 3 independent experiments is shown. (**d**) Fluorescence microscopy images of LCA (green), GNL (green) and DAPI (blue) staining in renal fibroblasts. Scale bars: 10 μm. (**e**) Representative confocal image of 2 independent experiments showing renal fibroblasts (from CL-11$^{-/-}$ mice) that had been incubated with rCL-11 (600ng/ml) for 24h and subjected to staining for CL-11 (red) and LCA (green) and nuclear marker DAPI (blue). Scale bars: 10 μm. (**f**) Proliferation rate of renal fibroblasts that had been pre-treated with buffer alone (Ctrl) or buffer

containing α-mannosidase (5 mM) or β-galactosidase (5 mM), and followed by incubation with rCL-11 (600 ng/ml). Data were analyzed by One-way ANOVA with Tukey's post-test (n=8 viewing fields from 2 cover glass/group). ***P*<0.005.

Figure 7. Kidney-specific deficiency of CL-11 protects against the development of tubulointerstitial fibrosis. Histological injury and renal fibrosis are shown for CL-11$^{+/+}$ mice transplanted with kidneys from CL-11$^{+/+}$ or CL-11$^{-/-}$ littermates. Kidney grafts were collected 7 days after transplantation. Pictures were taken at the cortical-medullary junction. (**a**) Left panel: representative images of PAS staining. Arrows illustrate injured tubules. Scale bars: 50 μm. Right panel: histological scores for renal tubular injury in the mice. Data were analysed by Unpaired two-tailed Student's *t* test (n=49-60 viewing fields from 7-8 mice/group, 0.49mm^2 per viewing field). ***, *P*<0.001. (**b**) Left panel: representative images of Sirius red staining. Arrows show collagen deposition. Scale bars: 50 μm. Right panel: quantification of Sirius red stained arears. Data were analysed by Unpaired two-tailed Student's *t* test (n=22-32 viewing fields from 3-4 mice/group). *, *P*<0.05.

Figure 8. Proposed mechanism by which CL-11 contributes to renal tubulointerstitial fibrosis. Based on our findings in this study and our published data in the study of acute injury, we propose that local production of CL-11 (by renal tubular epithelial cells and possibly by other cells) is upregulated by renal ischemia reperfusion. Locally produced CL-11: i) stimulates renal interstitial fibroblasts and causes cell proliferation and ECM production, ii) mediates influx of inflammatory cells into the kidney, these inflammatory cells produce pro-inflammatory and pro-fibrotic factors in response to debris stimulation, which increase tissue inflammation and fibrogenesis, iii) detects stress-induced L-fucose pattern on renal tubules to trigger complement activation that mediates renal tubular epithelial injury and production of pro-inflammatory and pro-fibrotic factors by tubular epithelial cells, which increase renal tissue inflammation and fibrogenesis.

Figure 1. Deficiency of CL-11 reduces tubule damage and renal function impairment in the late phase of renal IR

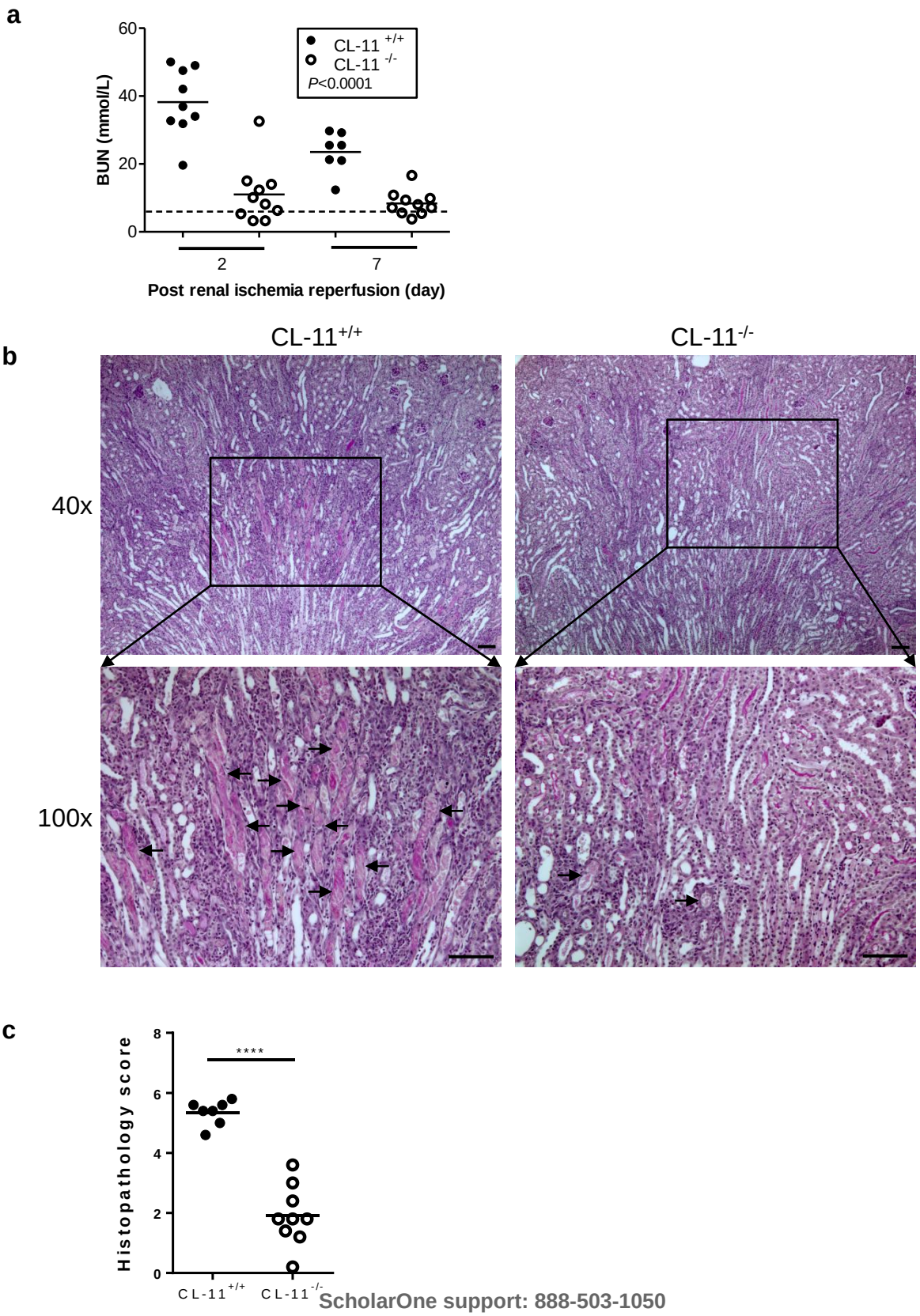

Figure 2. Deficiency of CL-11 reduces accumulation of ECM in the kidney following renal IR

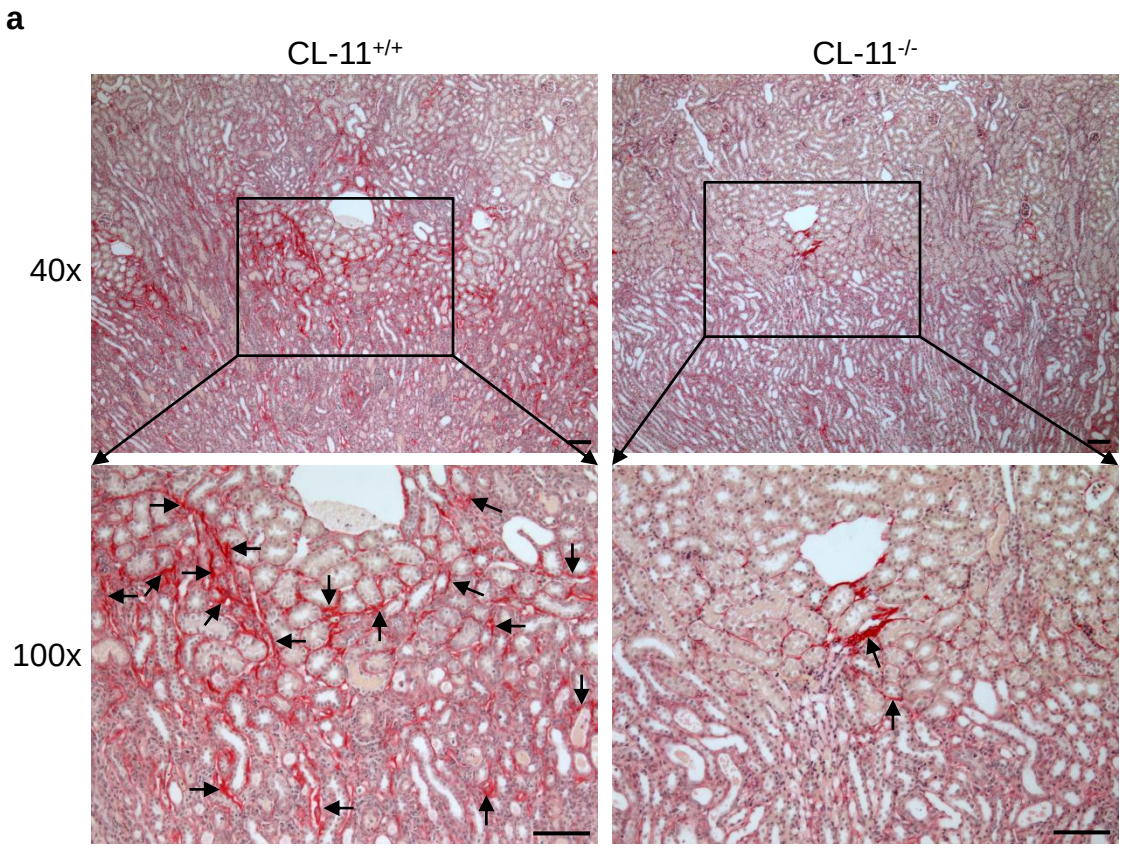

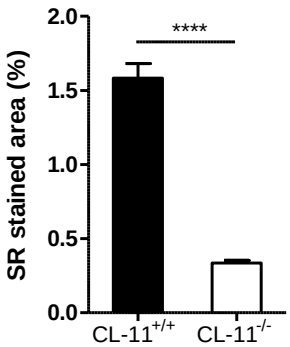

Figure 2. Deficiency of CL-11 reduces accumulation of ECM in the kidney following renal IR

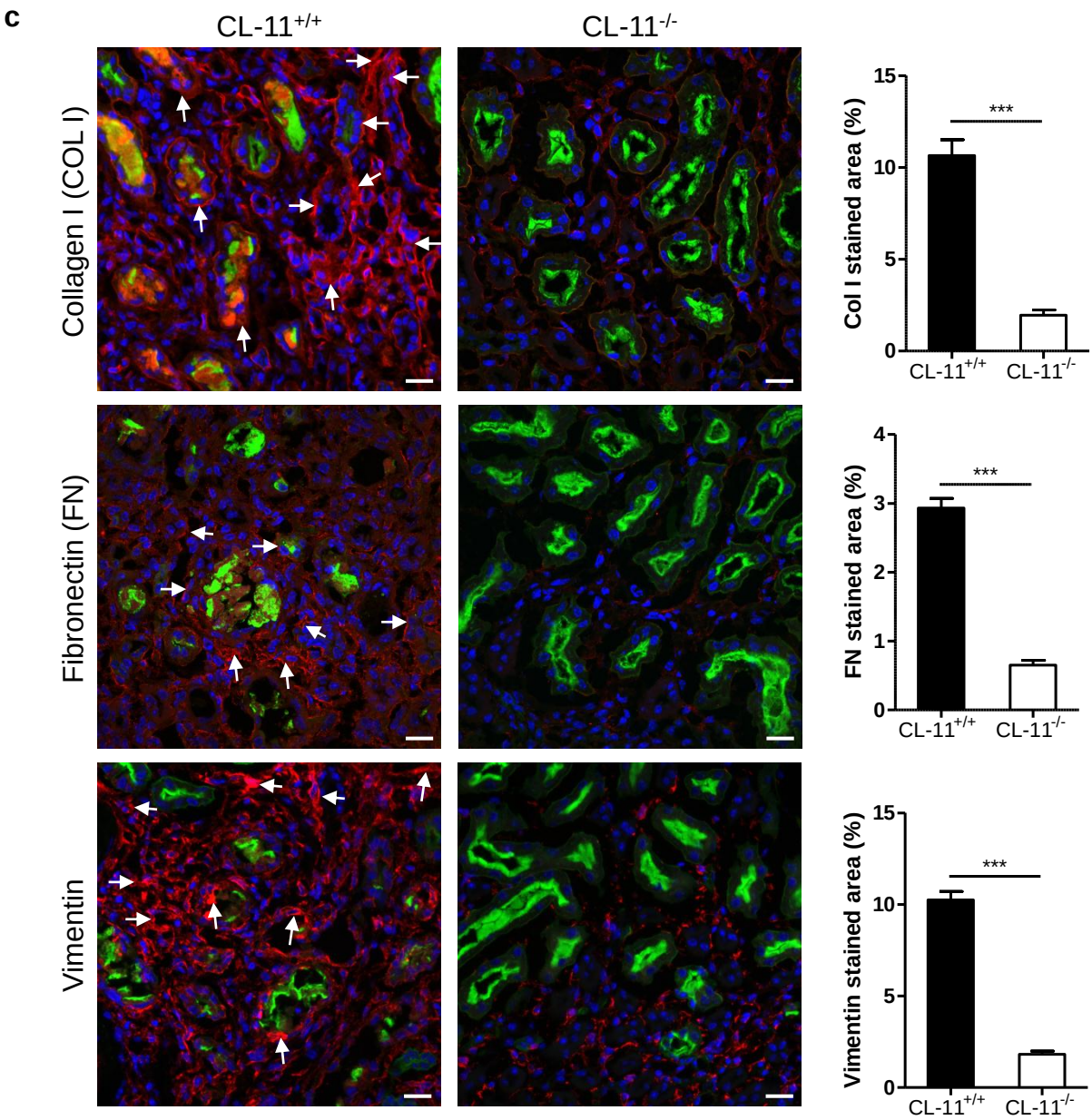

Figure 3. Deficiency of CL-11 reduces renal leukocyte infiltration following renal IR

a

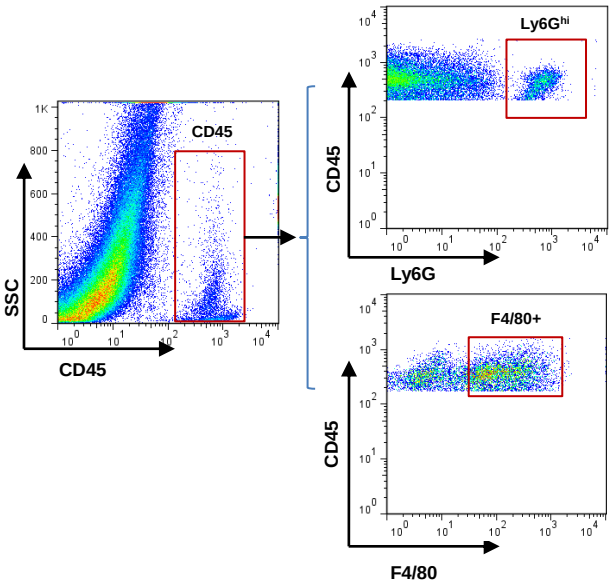

b

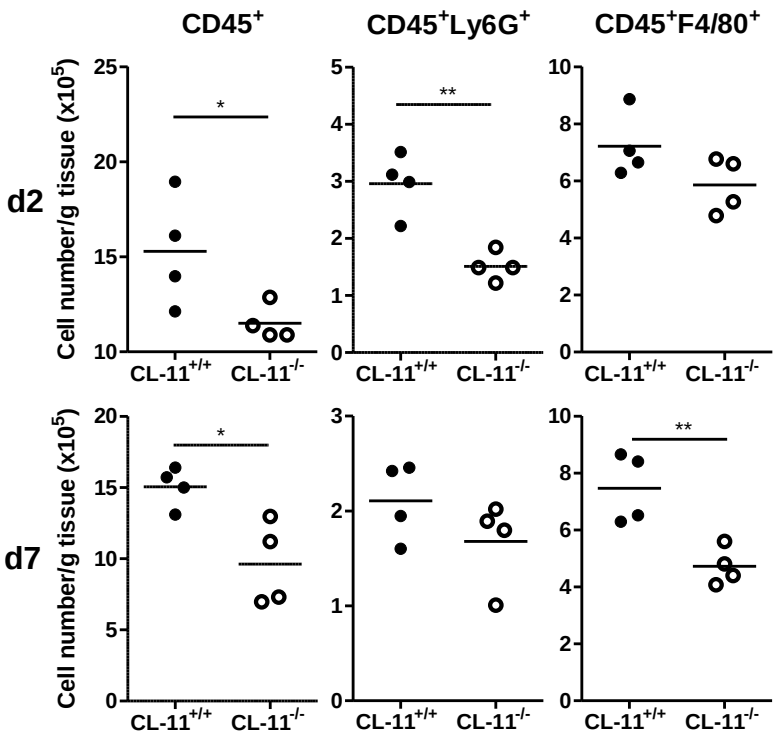

Figure 3. Deficiency of CL-11 reduces renal leukocyte infiltration following renal IR

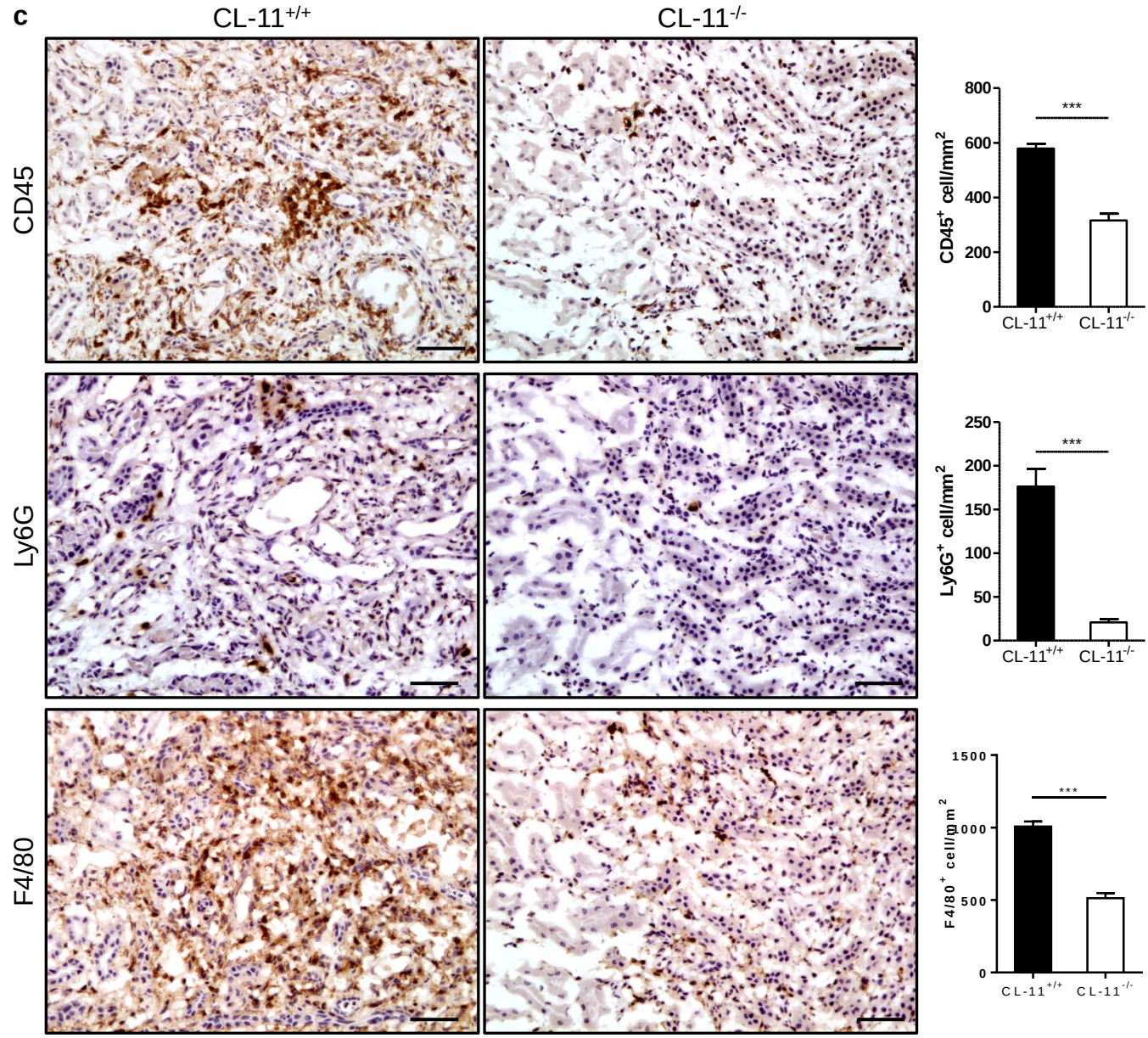

Figure 4. Deficiency of CL-11 reduces renal tissue inflammation and fibrogenesis following renal IR

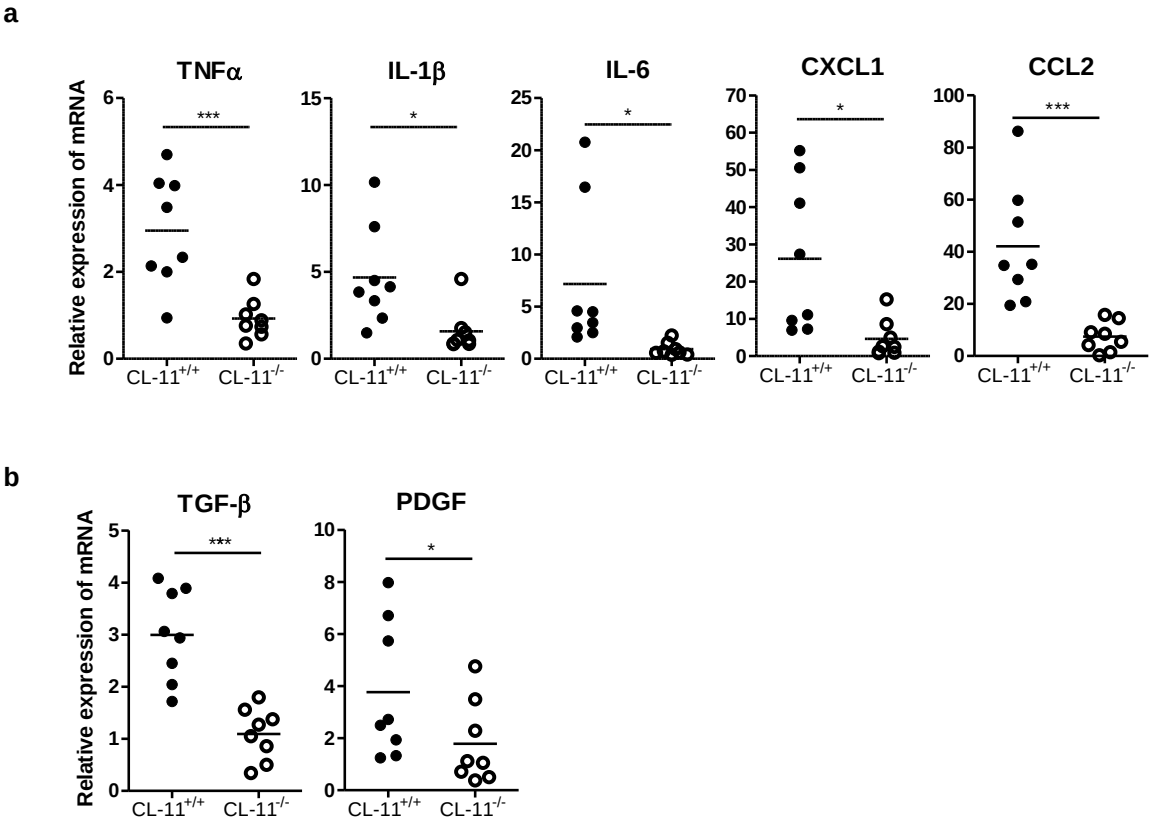

Figure 5. CL-11 promotes leukocyte migration *in vitro*

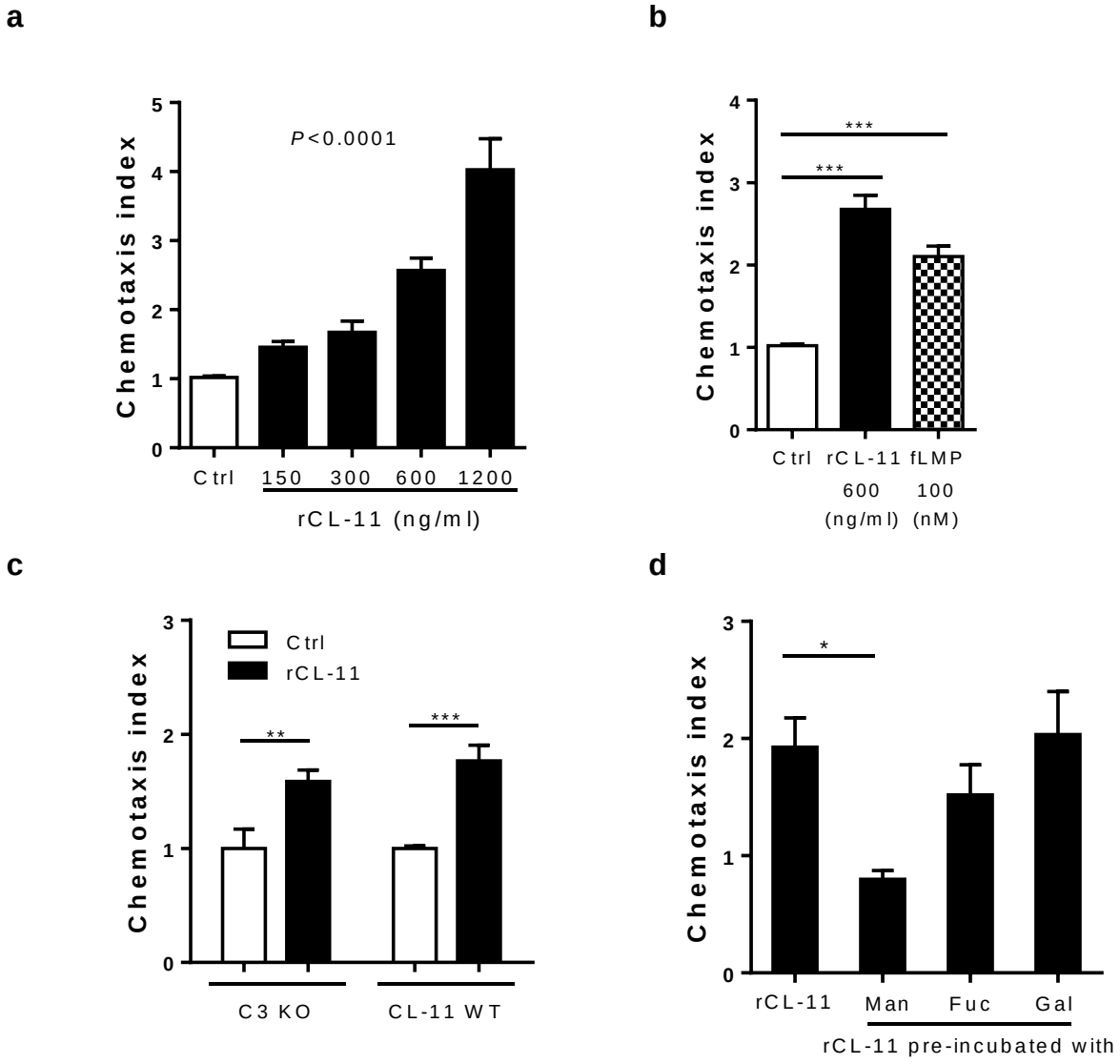

Figure 6. CL-11 stimulates renal fibroblast proliferation and ECM production

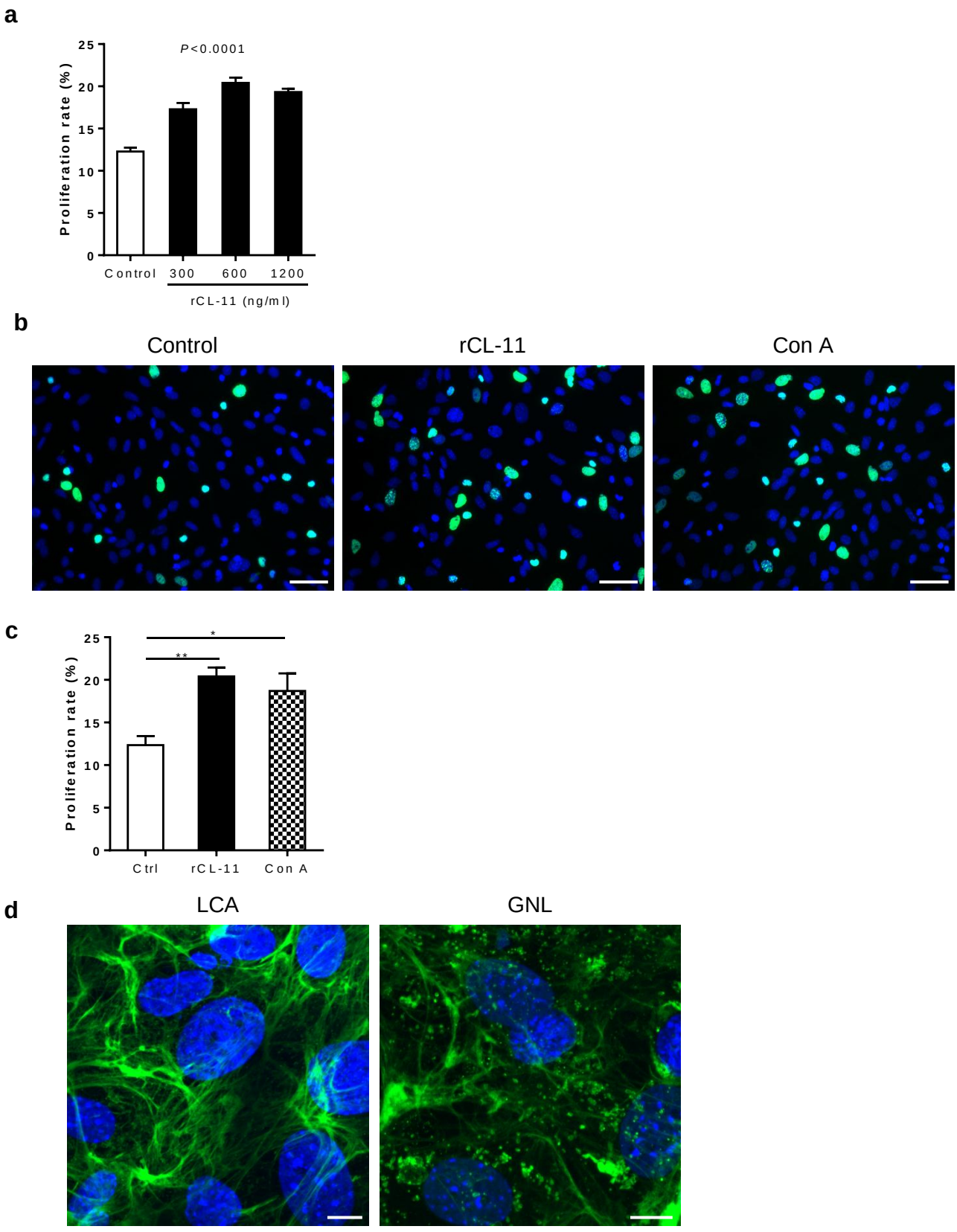

Figure 6. CL-11 stimulates renal fibroblast proliferation and ECM production

e

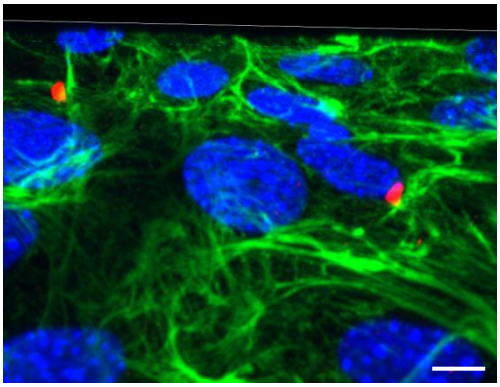

f

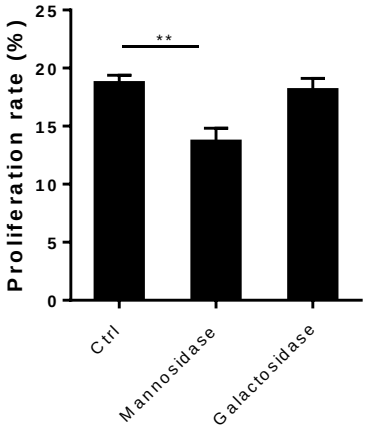

Figure 7. Kidney-specific deficiency of CL-11 protects against the development of tubulointerstitial fibrosis

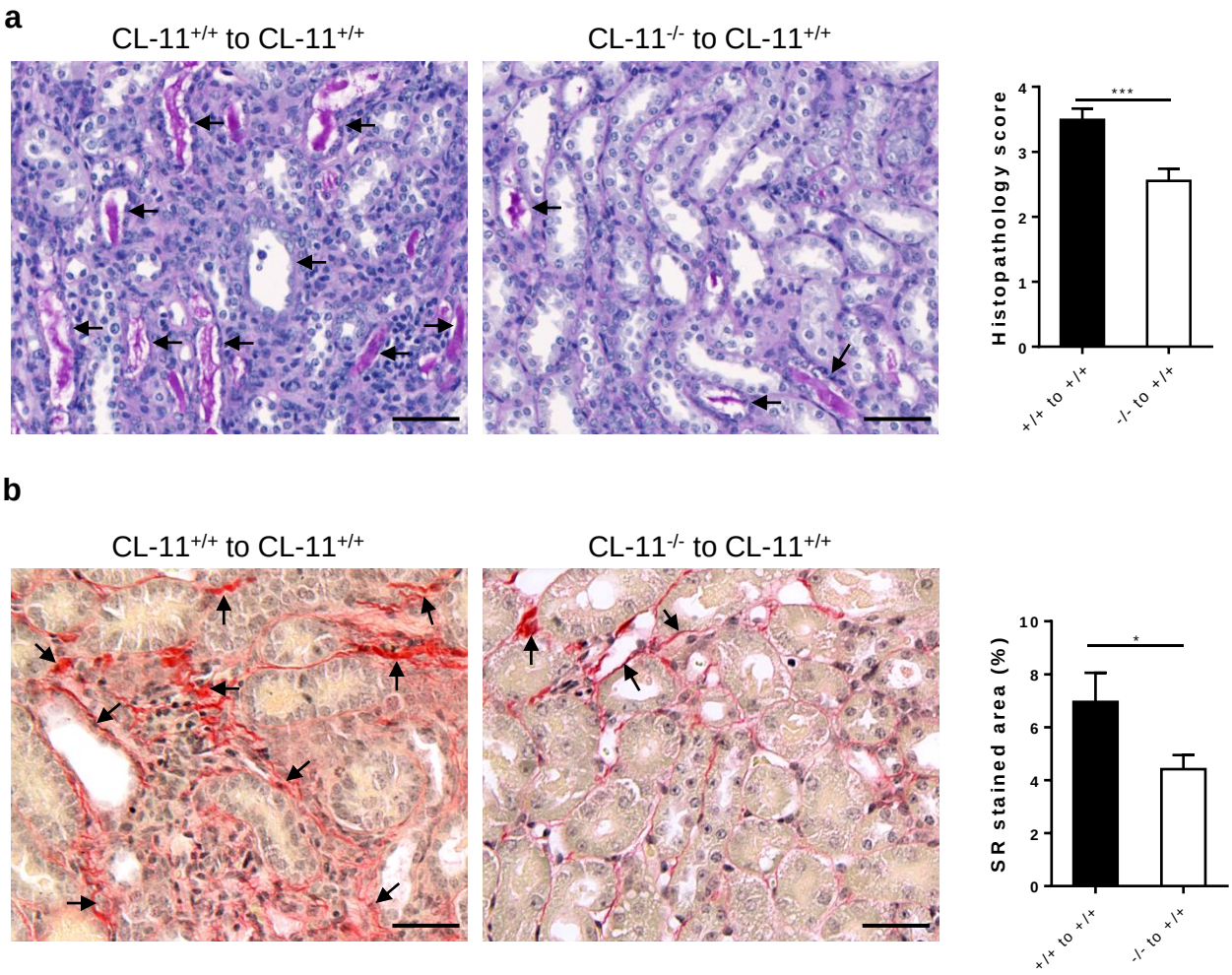

Figure 8. Proposed mechanism by which CL-11 contributes to renal tubulointerstitial fibrosis

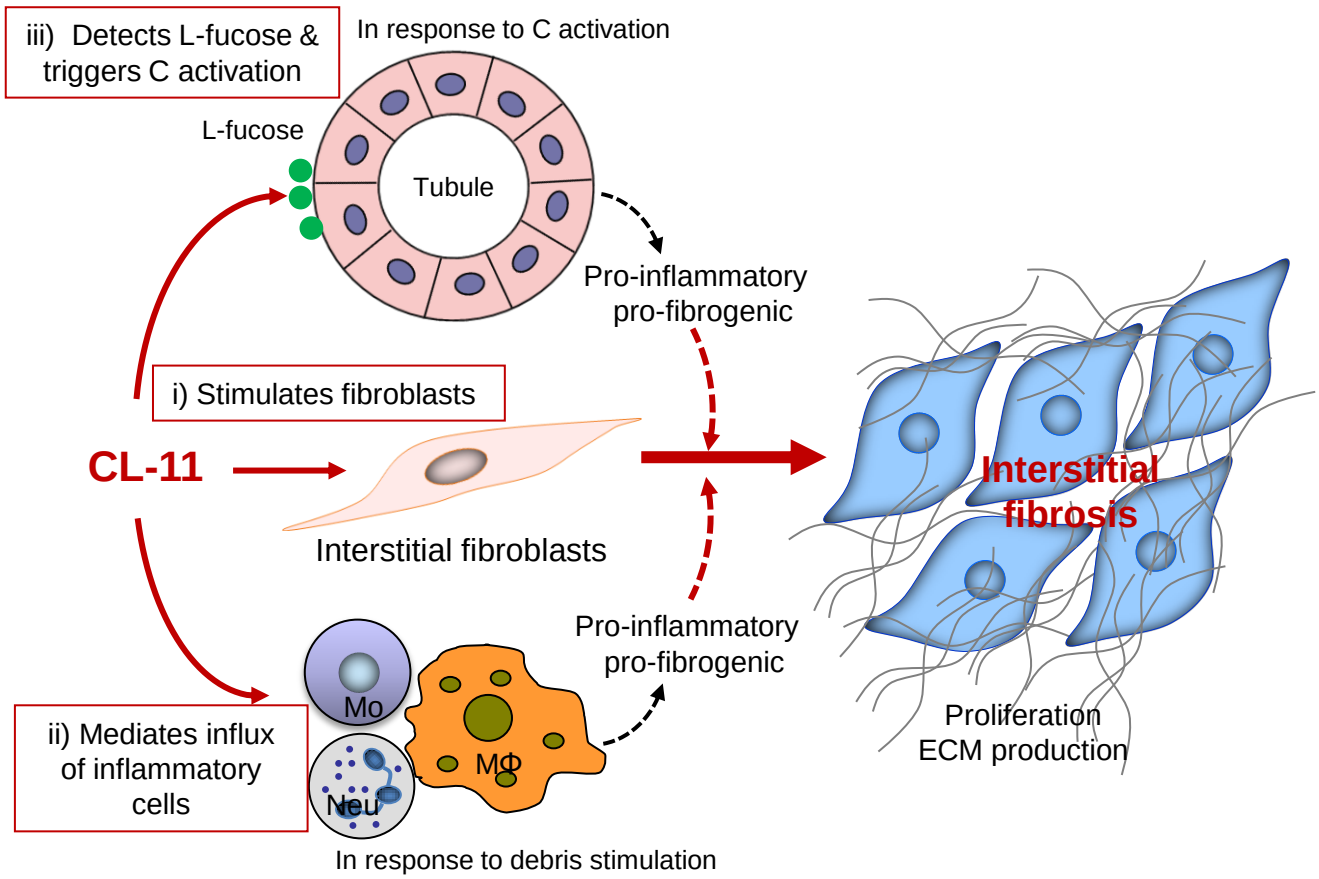

sFigure 1. Western blot analysis of rCL-11 and CL-11 WT mouse serum.

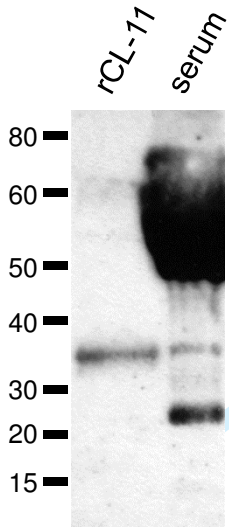

sFigure 1. Western blot analysis of rCL-11 and CL-11 WT mouse serum. rCL-11 (0.1 µg and CL-11 WT mouse serum (80 µg) were run in SDS-PAGE under a reducing condition, followed with western blot by using polyclonal goat anti-human COLEC11 Ab (1:300, Sant Cruz) and rabbit anti-goat HRP Ab (1:1000, Dako).

sFigure 2. Leukocytes and renal fibroblasts express a great amount of mannose moieties on the cell surface

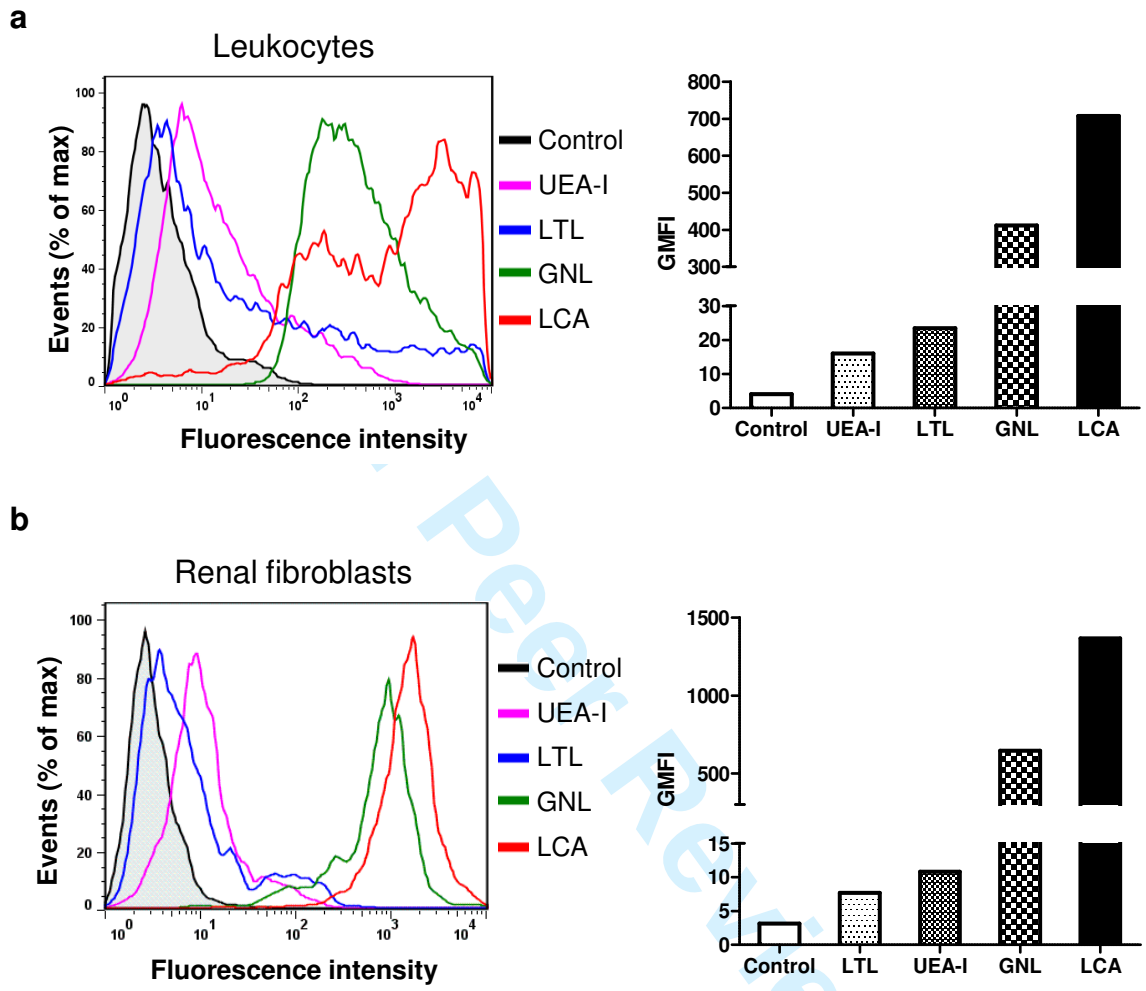

sFigure 2. Leukocytes and renal fibroblasts express a great amount of mannosyl residues on the cell surface. Peritoneal exudate cells (collected 24h after intraperitoneal injection of 1 ml of 3% thioglycollate) and renal fibroblasts were incubated without or with fluorescein labelled lectins, including Ulex Europaeus I (UEA-I), Lotus Tetragonolobus Lectin (LTL), Galanthus Nivalis Lectin (GNL) and Lens Culinaris Agglutinin (LCA), for 30 min and processed for flow cytometry. (**a**) histogram and quantification (shown as geometric mean of fluorescence intensity, GMFI) of the four lectins binding to peritoneal exudate cells. (**b**) histogram and quantification of the four lectins binding to renal fibroblasts.

sFigure 3. Characterisation of cultured renal fibroblasts by vimentin staining

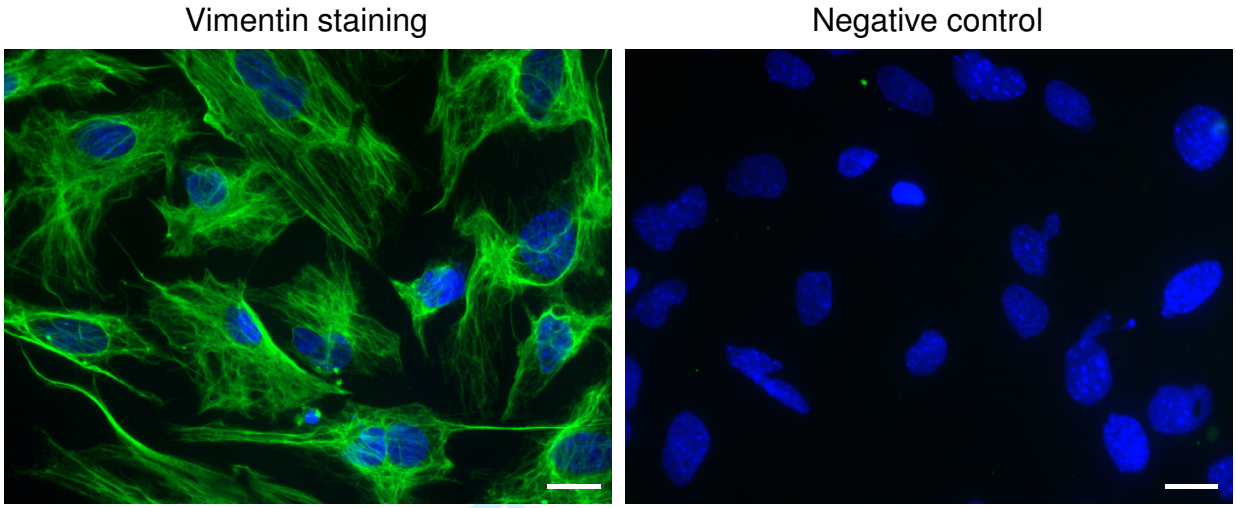

sFigure 3. Characterisation of cultured renal fibroblasts by vimentin staining. Representative fluorescence microscopy images of CL-11$^{-/-}$ renal fibroblast cells (of 2 independent experiments) that had been stained for vimentin (green) and nuclear marker DAPI (blue). Negative control was performed using the 2nd antibody alone. Scale bars: 20 µm.

sFigure 4. Deficiency of CL-11 does not influence C3d deposition in day 7 post-ischemic kidneys.

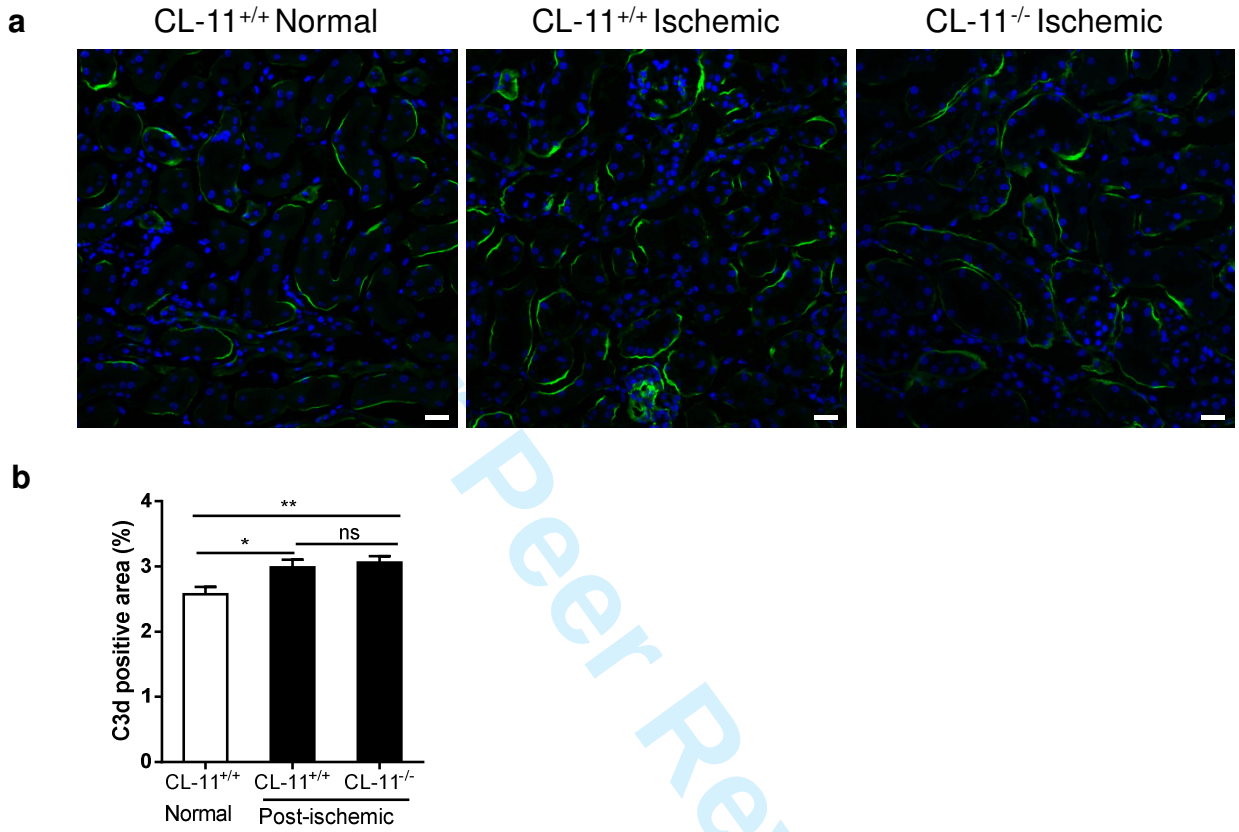

sFigure 4. Deficiency of CL-11 does not influence C3d deposition in day 7 post-ischemic kidneys. (**a**) Representative images of immunofluorescence staining of C3d in kidneys of normal CL-11$^{+/+}$ mice and ischemic CL-11$^{+/+}$ and CL-11$^{-/-}$ mice at day 7 post renal ischemia reperfusion. (**b**) Quantifications of C3d in kidneys corresponding to the mice represented in **a**. Data are shown as mean ± SEM and were analysed by One-way ANOVA with Tukey's post-test (n=20 viewing fields from 4 mice/group). *, P<0.05; **, P<0.001; ns, no significant. Scale bars: 20 µm.

sFigure 5. Detection of C3d deposition in renal fibroblast cultures

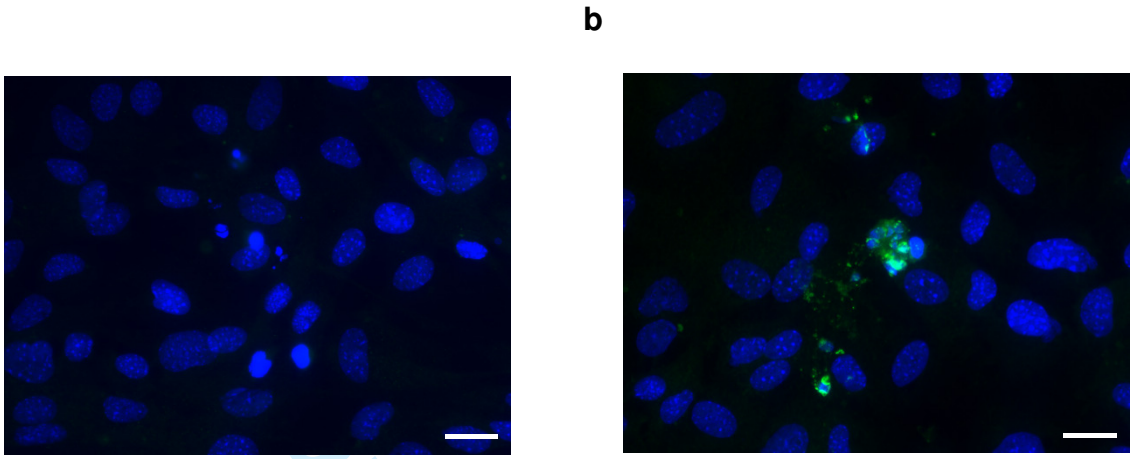

sFigure 5. Detection of C3d deposition in renal fibroblast cultures. Fluorescence microscopy images of immunochemical staining of C3d (green) and DAPI (blue) in renal fibroblasts cultured from CL-11$^{-/-}$ mice. Cells were incubated with recombinant CL-11 (rCL-11, 600ng/ml) for 48 h or 20% CL-11$^{+/+}$ mouse serum for 30 min, followed by fixation with 4% paraformaldehyde. They were then stained with rabbit polyclonal anti-human C3d and goat anti-rabbit Alexa Fluor 488. (**a**) Renal fibroblasts treated with rCL-11. (**b**) Renal fibroblasts treated with 20% CL-11$^{+/+}$ mouse serum. Scale bars: 20 µm.

sFigure 6. Tubular debris stimulates macrophages to secrete pro-inflammatory factors and subsequently increases fibroblast proliferation

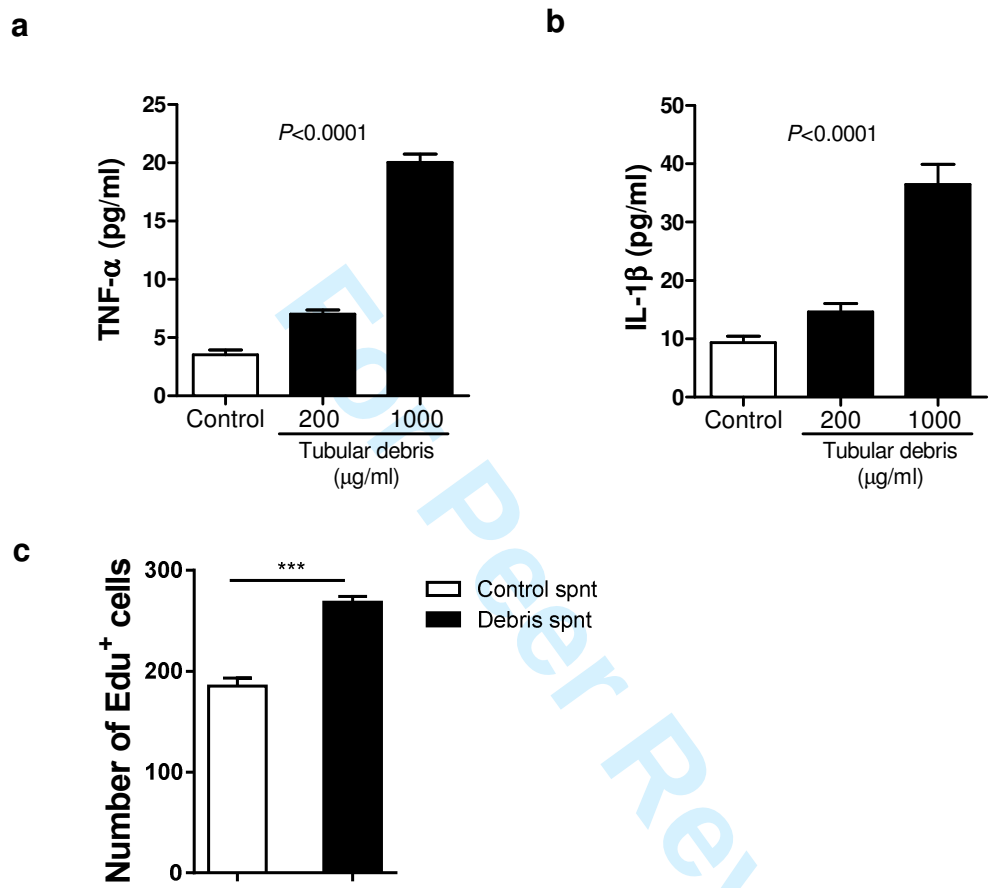

sFigure 6. Tubular debris stimulates macrophages to secrete pro-inflammatory factors, which increase fibroblast proliferation. Peritoneal exudate cells, mainly macrophages, were collected from CL-11$^{+/+}$ mice 3 days after intraperitoneal injection of thioglycollate. They were incubated without or with tubular debris (200 ng/ml or 1000 ng/ml) for 24 h. Half of supernatants were used to measure TNF-α and IL-1β concentrations by ELISA. The other half was incubated with renal fibroblasts for 2 days and followed by EdU labelling. (**a, b**) TNF-α and IL-1β levels. Data are shown as mean ± SEM and were analysed by One-way ANOVA (n=4 per group), by comparing the control and renal tubular debris stimulated. (**c**) Counting of EdU-positive cells. Data are shown as mean ± SEM and were analysed by Unpaired two-tailed Student's *t* test (n=4 per group). ***, *P*<0.0001. (**a-c**) A representative of 2 individual experiments is shown.

sFigure 7: Renal fibrosis and tubule damage in $C3^{-/-}$ and $C3^{+/+}$ mice following IR injury

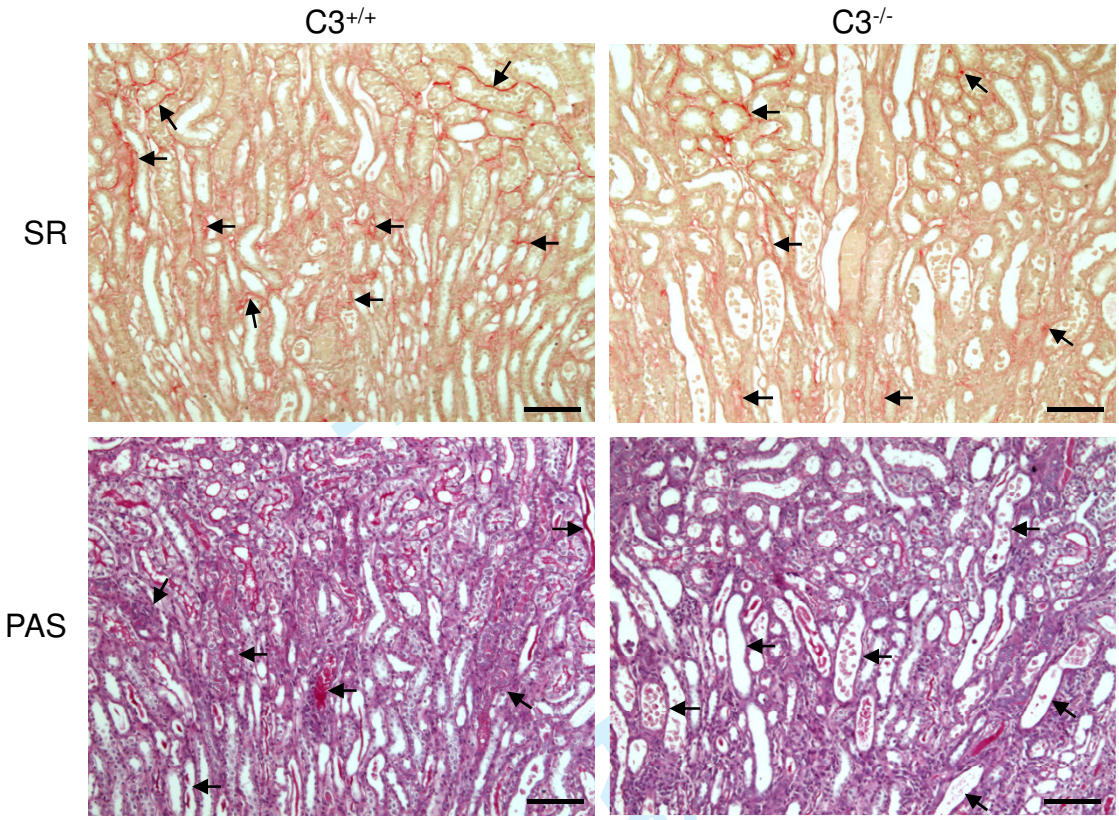

sFigure 7: Renal fibrosis and tubule damage in $C3^{-/-}$ and $C3^{+/+}$ mice following IR injury. Representative images of Sirius red and PAS staining in $C3^{+/+}$ and $C3^{-/-}$ mouse kidneys at day 7 post renal ischemia (30 min) reperfusion injury, taken at the cortical medullary junction. Arrows indicate positive stained arears and injured tubules. Scale bars: 100 µm.

Supplementary Table 1

PCR primer sequences and product sizes

Primer*	Oligonucleotide Sequence (5' → 3')	Product Size (bp)	Gene bank code
18S-1 18S-2	ATC CCT GAG AAG TTC CAG CA CCT CTT GGT GAG GTC GAT GT	153	NM_011296.1
TNF-α-1 TNF-α-2	TGA GCA CAG AAA GCA TGA TCC GCC ATT TGG GAA CTT CTC ATC	200	NM_013693.3
IL6-1 IL6-2	GTT CTC TGG GAA ATC GTG GA GGA AAT TGG GGT AGG AAG GA	339	NM_031168
CXCL1-1 CXCL1-2	TGA AGC TCC CTT GGT TCA GA TGC ACT TCT TTT CGC ACA AC	361	NM_008176.3
CCL2-1 CCL2-2	GGC TCA GCC AGA TGC AGT TA ATT TGG TTC CGA TCC AGG TT	219	NM_011333.3
TGF-β-1 TGF-β-2	AAT ACG TCA GAC ATT CGG GAA CCG GGT TGT GTT GGT TGT AGA G	640	NM_011577
PDGF-1 PDGF-2	TAT GAA ATG CTG AGC GAC CA GAT CGA TGA GGT TCC GAG AG	250	ENSMUST00000000500
Collagen I -1 Collagen I -2	TGA CTG GAA GAG CGG AGA GT GTT CGG GCT GAT GTA CCA GT	151	OTTMUST00000004184
Fibronectin-1 Fibronectin-2	GAA GTC GCA AGG AAA CAA GC GCA TCG TAG TTC TGG GTG GT	393	NM_010233

* Primer-1 is identical to the coding strand; primer-2 is complementary to the coding strand.

Collectin-11 is required for the development of renal tubulointerstitial fibrosis

METHODS

Bilateral renal ischemia reperfusion injury was induced in CL-11$^{+/+}$ and CL-11$^{-/-}$ mice and tubulointerstitial fibrosis was assessed by evaluation of collagen deposition and tubule damage 7 days later.

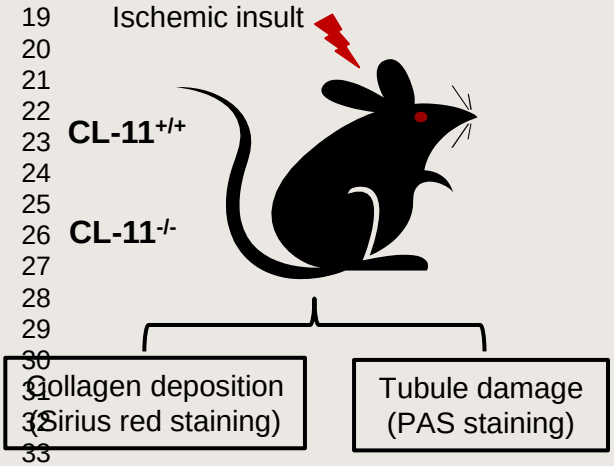

RESULTS

CL-11 deficiency reduced collagen deposition in the peritubular interstitium and tubule damage.

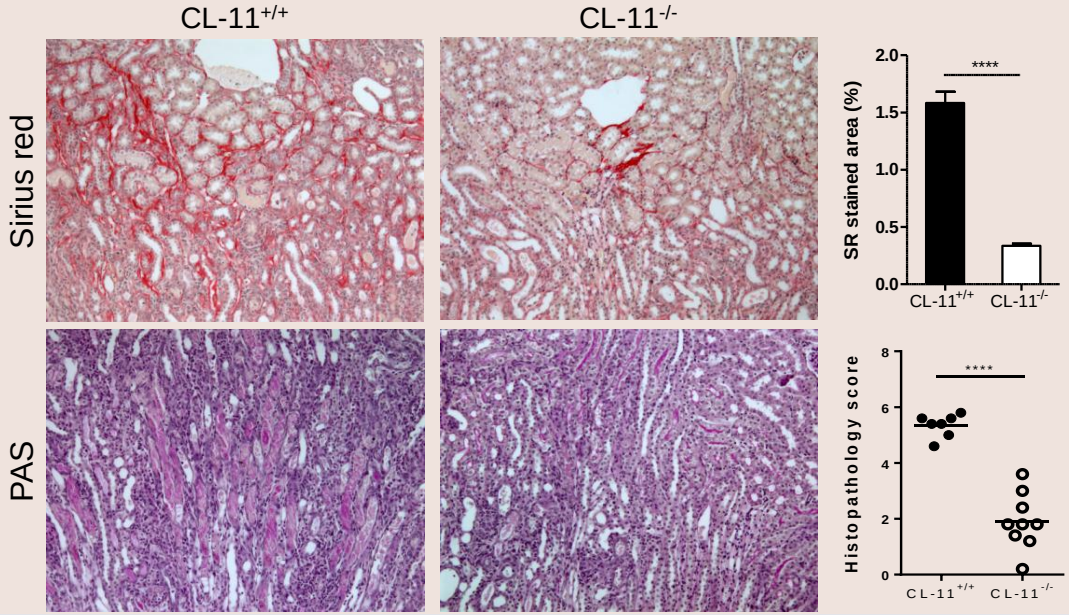

CONCLUSION

CL-11 plays a pathogenic role in the development of renal tubulointerstitial fibrosis in chronic kidney injury.

Weiju Wu, Chengfei Liu, Conrad A. Farrar, Liang Ma, Xia Dong, Steven S. Sacks, Ke Li, & Wuding Zhou. Collectin-11 is required for the development of renal tubulointerstitial fibrosis. J Am Soc Nephrol. Published ahead of print July 27, 2017. dio:

doi: 10.1681/ASN.

JASN
JOURNAL OF THE AMERICAN SOCIETY OF NEPHROLOGY

Significant statement

Collectin 11 (CL-11) is known to play important roles in embryonic development and host defence, as well as acute renal injury. However, the impact of CL-11 on chronic inflammation and tissue fibrosis is presently unknown. This manuscript reports a previously unknown pathogenic role for CL-11 in the development of tubulointerstitial fibrosis. It also defines two novel cellular mechanisms by which CL-11 promotes inflammatory cell migration and stimulates renal fibroblast proliferation that contribute to the development of tubulointerstitial fibrosis. This study provides new insight into pathogenesis of tubulointerstitial fibrosis and opens new avenues for studying the roles of CL-11 in renal fibrosis mediated by other causes and tissue fibrosis in other organs.